**Table 1.** Incidence of EGFR Mutations and Clinical and Pathologic Features

| Variable | EGFR Mutation | | EGFR Wild-Type | *P* |
|---|---|---|---|---|
| | No. of Patients | % | | |
| All cases | 33 | 56 | 26 | |
| Sex | | | | |
| Male | 14 | 44 | 18 | .0402 |
| Female | 19 | 70 | 8 | |
| Age, years | | | | |
| ≤ 64 | 22 | 55 | 18 | .8342 |
| > 64 | 11 | 58 | 8 | |
| Histologic type | | | | |
| Adenocarcinoma | 32 | 64 | 18 | .0033 |
| Nonadenocarcinoma | 1 | 11 | 8 | |
| Squamous cell carcinoma | 0 | 0 | 5 | |
| Large-cell carcinoma | 0 | 0 | 3 | |
| Adenosquamous carcinoma | 1 | 100 | 0 | |
| Smoking status | | | | |
| Never smoker | 20 | 71 | 8 | .0227 |
| Former or current smoker | 13 | 42 | 18 | |
| Stage | | | | |
| I-II | 12 | 50 | 12 | .4472 |
| III-IV | 21 | 60 | 14 | |

Abbreviation: EGFR, epidermal growth factor receptor.

recurrence was almost identical in patients with *EGFR* mutations (362 days) and in those without *EGFR* mutations (363 days; $P = .8265$).

### Clinical Improvement After Gefitinib Treatment

Forty-one of 59 patients had measurable disease at recurrence with imaging studies. Of these, 20 showed appreciable tumor shrinkage after gefitinib treatment, whereas 17 tumors increased in size, and there was no change in tumor size in four patients. All of these 20 tumors (pulmonary metastases in 11, pleural disseminated nodules in two, hepatic metastases in two, mediastinal lymph node swelling in two, brain metastases in two, and chest wall tumor in one) showed at least a 30% decrease in diameter. Figure 2 shows representative imaging studies. A computed tomography scan of the chest in patient L703 (73-year-old woman, adenocarcinoma) showed masses in the right-lower lobe and marked improvement 8 weeks after gefitinib initiation. A computed tomography scan of the liver in patient L1492 (52-year-old woman, adenocarcinoma) showed masses in the right lobe of the liver and dramatic improvement 10 days after gefitinib initiation. A large chest-wall mass in the left back of patient L1362 (62-year-old man, adenosquamous carcinoma) before gefitinib treatment almost disappeared 13 weeks after gefitinib initiation. A left-lung tumor in patient L1171 (70-year-old woman, adenocarcinoma) was smaller 6 weeks after gefitinib initiation.

CEA was above the upper normal limit (5 ng/mL) at baseline in 32 patients. Serum CEA level decreased to $< 10\%$, $< 50\%$, and to $> 50\%$ of the baseline level in three, 12, and five patients, respectively, whereas CEA level increased in 12 patients. When we combined the results of imaging studies with CEA and judged according to our criteria, gefitinib treatment was effective in 26 (52%), not effective in 24 (48%), and not assessable in nine patients (Table 2). There was a good correlation between these two examinations. The imaging studies and change in CEA levels did not conflict in any patients. In 17 patients with measurable diseases and whose baseline CEA level was elevated, the CEA level decreased in all 11 patients showing tumor shrinkage and increased in all five patients showing tumor growth, except for one patient whose tumors showed no change in size ($P < .001$, Fisher's exact test), supporting the validity of our criteria.

We searched for a relation between gefitinib effectiveness and various clinical and pathologic features (Table 2). Never-smokers and patients with adenocarcinoma had a significantly higher incidence of gefitinib effect. However, we could not detect significant difference in gefitinib sensitivity by sex or presence of prior chemotherapy, probably because of the small sample size, although there was a trend that female and chemotherapy-naïve patients were more responsive.

### Relationship Between Clinical Response to Gefitinib Treatment and EGFR Mutations

The incidence of *EGFR* mutations in terms of response to gefitinib treatment as judged by imaging studies and CEA levels is shown in Table 3. Of 20 patients who showed tumor shrinkage, 19 (95%) had mutations of the *EGFR* gene. On the other hand, two (12%) of 17 patients whose tumors grew after gefitinib treatment harbored *EGFR* mutations ($P < .001$, Fisher's exact test). In Figure 2, patient L703, L1492, and L1362 had *EGFR* mutations (delE746-A750, L858R, and E746-S752insA, respectively). Of three, 12, and five patients whose CEA level decreased to less than 10%, less than 50%, and to more than 50% of the baseline level after gefitinib treatment, three (100%), 10 (83%), and four (80%) had *EGFR* mutations, respectively. On the other hand, of 12 patients whose CEA level increased, three (25%) had *EGFR* mutations ($P = .004$, Fisher's exact test).

When we used our criteria combining the results of imaging studies with CEA, gefitinib was effective in 24 (83%) of 29 patients with *EGFR* mutations, whereas it was effective only in two (10%) of 21 patients without *EGFR* mutations ($P < .0001$; Table 2). There were three patients with *EGFR* mutations (two with L858R and one with G719A) whose CEA level increased after gefitinib treatment but did not have measurable diseases. There were also two patients with *EGFR* mutations, one with L858R+E709H and one with I744-K745 ins KIPVAI whose tumor progressed.

Logistic regression analysis (Table 4) showed that *EGFR* mutation was the only significant factor contributing to gefitinib sensitivity.

On the other hand, patient L1171, who showed a decrease in size of multiple pulmonary metastatic nodules

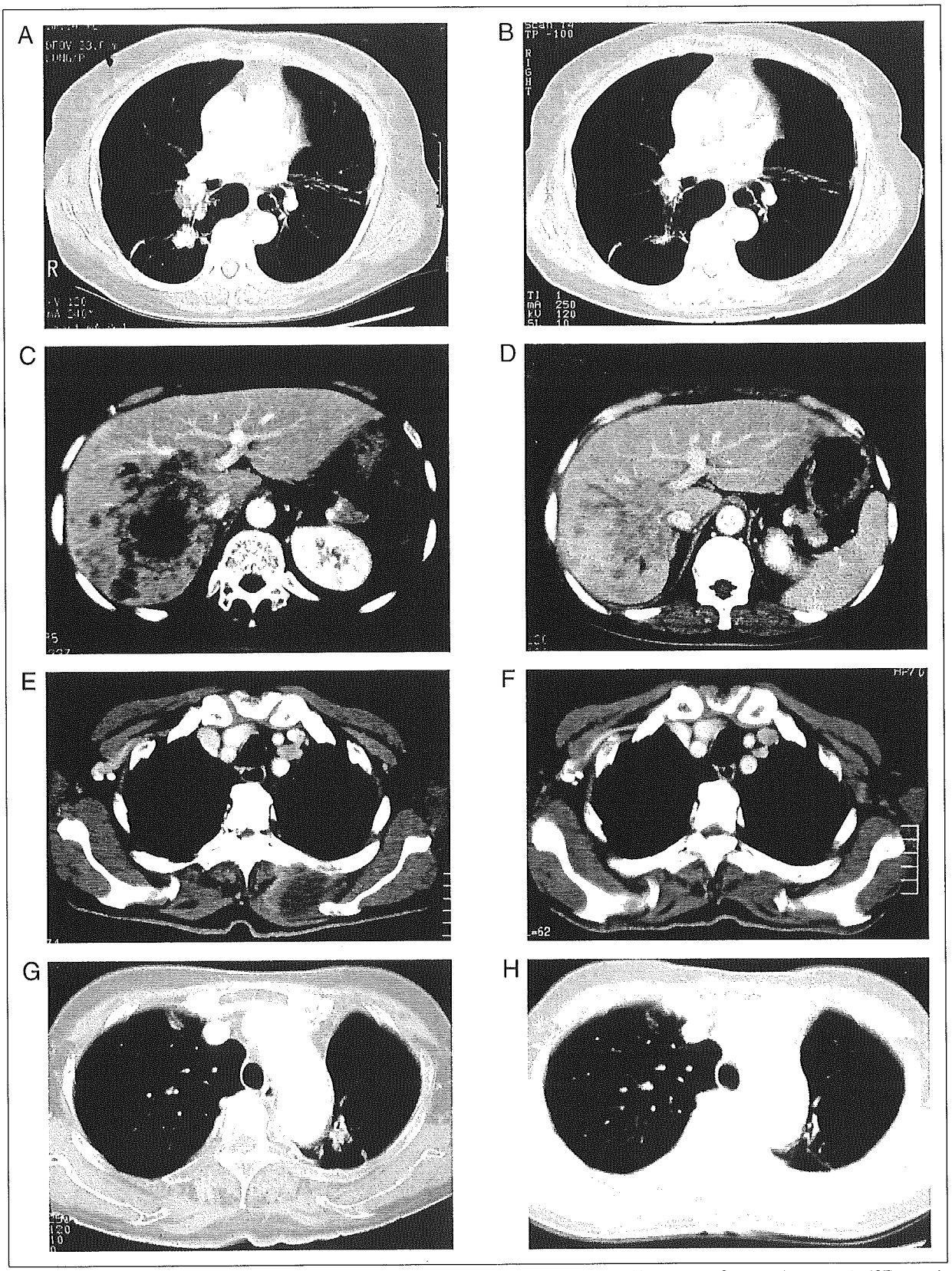


**Fig 2.** Examples of the response to gefitinib in representative four patients with recurrent non–small-cell lung cancer. Computed tomography (CT) scans before gefitinib treatment (A, C, E, G) and after the gefitinib was initiated (B, D, F, H) are shown. CT scans of patient L703 (A, B), patient L1492 (C, D), patient L1362 (E, F), and patient L1171 (G, H).

**Table 2.** Relation Between Gefitinib Effectiveness and Various Clinical and Pathologic Features

| Variable | Effective: No. of Patients | Effective: %* | Not Effective | Not Assessable | P† |
|---|---|---|---|---|---|
| All patients | 26 | 52 | 24 | 9 | |
| Sex | | | | | |
| Male | 11 | 41 | 16 | 5 | .0842 |
| Female | 15 | 65 | 8 | 4 | |
| Smoking status | | | | | |
| Never-smoker | 17 | 68 | 8 | 3 | .0235 |
| Former or current smoker | 9 | 36 | 16 | 6 | |
| Histologic type | | | | | |
| Adenocarcinoma | 25 | 58 | 18 | 7 | .0313 |
| Nonadenocarcinoma | 1 | 14 | 6 | 2 | |
| Prior chemotherapy | | | | | |
| Present | 17 | 47 | 19 | 4 | .2782 |
| Absent | 9 | 64 | 5 | 5 | |
| EGFR mutation | | | | | |
| Mutation | 24 | 83 | 5 | 4 | < .0001 |
| Deletion | 16 | 100 | 0 | 1 | .0108‡ |
| Insertion | 0 | 0 | 1 | 0 | |
| Point mutation | 8 | 67 | 4 | 3 | |
| Wild-type | 2 | 10 | 19 | 5 | |

Abbreviation: EGFR, epidermal growth factor receptor.
*Percentages were calculated excluding patients who were not assessable.
†*P* values were calculated excluding patients who were not assessable.
‡*P* value for Fisher's exact test comparing deletion mutants with the other mutants.

(Figs 2G and H) and a decrease in CEA level from 16.8 to 4.3 ng/mL, did not have *EGFR* mutations. In this patient, we extended our search for mutations to exons 22 and 23 of the *EGFR* gene, and still found none. Another patient without *EGFR* mutation in whom gefitinib was effective was a 59-year-old man who showed a decrease in serum CEA level from 10.6 to 1.5 ng/mL after 2 weeks of gefitinib treatment; this low level of CEA was maintained at least for 7 months.

When we further analyzed gefitinib response by classes of *EGFR* mutation, we found that there was a difference of response between patients with deletion mutations and those with the other types of mutations. Gefitinib was effective in all 16 patients with deletions, and effective in eight of 13 with other types of mutation ($P = .0108$).

### *Effect of* EGFR *Mutation on Patient Survival After Gefitinib Treatment*

Patients with *EGFR* mutations survived for a significantly longer time calculated from the day of gefitinib initiation than those without *EGFR* mutations ($P = .0053$, log-rank test; Fig 3). Likewise, 26 gefitinib responders survived for a longer time than 24 nonresponders ($P = .0320$, log-rank test; not shown). Multivariate analysis revealed that *EGFR* mutation was the only factor that significantly and independently affected overall survival (Table 5). *EGFR* mutation class did not affect overall survival (not shown).

## DISCUSSION

Recurrence after complete resection of NSCLC often presents as a form of distant metastases.[20] In clinical practice, chemotherapy is given to these patients except for a small number in whom re-resection of the tumor is indicated. Many studies have shown that chemotherapy prolongs survival and improves quality of life in unresectable stage IV tumors.[21] However, patients with unresectable tumors and patients with recurrent diseases may not be the same. There have been no large-scale randomized clinical trials addressing whether chemotherapy improves survival of patients with recurrence. Yoshino et al[22] found that chemotherapy for recurrence only tended to prolong survival in 118 of 468 consecutive patients who had recurrence after pulmonary resections. After introduction of gefitinib to clinical practice in 2002 in Japan, some patients with recurrent disease showed dramatic responses to gefitinib treatment, but many others did not respond. It has been unclear which patients respond to gefitinib and also whether gefitinib treatment prolongs survival in these patients.

Recent studies have showed striking correlation between gefitinib sensitivity and *EGFR* mutations both in vitro and in clinical studies.[15-17] Because this study was a retrospective analysis of response to gefitinib prescribed as routine care, judgment of gefitinib effectiveness tended to be less strict than that in a prospective clinical trial. Yet, changes in serum CEA level never conflicted with imaging studies. We were able to confirm a relation between *EGFR*

**Table 3.** Response to Gefitinib Treatment in 59 Patients With Recurrent Disease

| CEA Level | Imaging Results: Shrinkage | No Change | Not Measurable | Growth | Total |
|---|---|---|---|---|---|
| Decreased | | | | | |
| <10% of the baseline | **3 (3)** | | | | 3 (3) |
| <50% of the baseline | **6 (5)** | **1 (1)** | **5 (4)** | | 12 (10) |
| >50% of the baseline | **2 (2)** | | *3 (2)* | | 5 (4) |
| Not assessable | **9 (9)** | *3 (1)* | *3 (1)* | 12 (2) | 27 (13) |
| Elevated | | | 7 (3) | 5 (0) | 12 (3) |
| Total | 20 (19) | 4 (2) | 18 (10) | 17 (2) | 59 (33) |

NOTE. Numbers in bold indicate that gefitinib treatment resulted in clinical improvement in these patients; numbers with underlines indicate the treatment resulted in progression of the disease; numbers in parentheses show number of patients with EGFR mutations in each category; and italicized numbers indicate that gefitinib treatment could not be assessed.
Abbreviations: EGFR, epidermal growth factor receptor; CEA, carcinoembryonic antigen.

**Table 4.** Logistic Regression Analysis of Various Factors That Predict EGFR Effectiveness

| Variable | Odds Ratio | 95% CI | *P* |
|---|---|---|---|
| Sex | | | |
| Male/female | 1.139 | 0.130 to 9.953 | .9063 |
| Smoking status | | | |
| Never/former/current | 1.496 | 0.165 to 13.535 | .7202 |
| Histologic type | | | |
| Adenocarcinoma/ nonadenocarcinoma | 1.727 | 0.091 to 33.33 | .7159 |
| Prior chemotherapy | | | |
| Yes/no | 0.427 | 0.060 to 3.027 | .3948 |
| EGFR mutation | | | |
| Mutant/wild-type | 40.000 | 6.024 to 2750 | < .0001 |

Abbreviation: EGFR, epidermal growth factor receptor.

mutations and gefitinib sensitivity in a slightly different clinical setting. We correlated *EGFR* mutations found in specimens taken at the time of surgery with response to gefitinib, often after several courses of cytotoxic chemotherapy for recurrent disease. Multivariate analysis revealed that *EGFR* mutation was the only independent predictor for gefitinib response among several allegedly contributing factors. As in previous studies, *EGFR* mutation was not a perfect predictor of gefitinib effectiveness.[15-17] Two patients without *EGFR* mutations showed response to gefitinib. It is not clear at this time whether *EGFR* mutations are present in other parts of the gene or whether mechanisms other than *EGFR* mutations govern sensitivity in these patients.

We found a significant difference in gefitinib sensitivity according to classes of *EGFR* mutations. All 16 patients with deletion mutants responded to gefitinib, compared with eight of 12 patients with other mutations ($P$ = .0108). It is not clear whether this difference is based on differences in biologic activity of these mutant proteins.

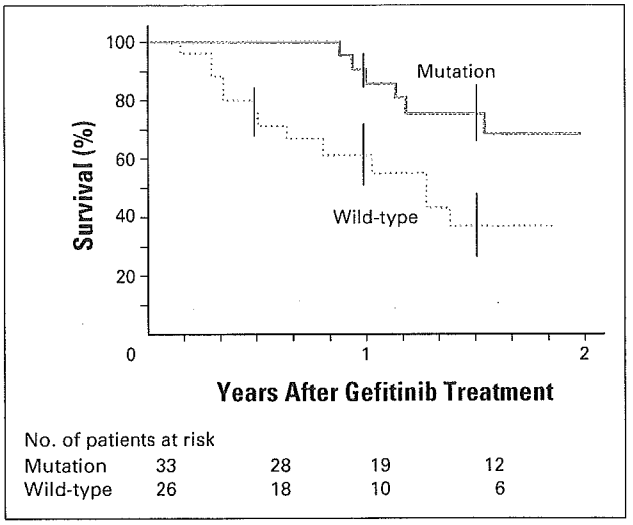


**Fig 3.** Effect of epidermal growth factor receptor mutations on survival, calculated from the day of initiating gefitinib treatment in patients who had recurrent disease after surgery ($P$ = .0053, log-rank test).

**Table 5.** Cox Proportional Hazards Model for Survival Analysis

| Variable | Hazard Ratio | 95% CI | *P* |
|---|---|---|---|
| Sex | | | |
| Female/male | 0.359 | 0.068 to 1.900 | .2280 |
| Smoking status | | | |
| Never/former/current | 0.511 | 0.092 to 2.854 | .4445 |
| Histologic type | | | |
| Adenocarcinoma/ nonadenocarcinoma | 0.335 | 0.095 to 1.184 | .0894 |
| Prior chemotherapy | | | |
| Yes/no | 0.653 | 0.222 to 1.923 | .4397 |
| Stage | | | |
| I-II/III-IV | 0.848 | 0.322 to 2.232 | .7380 |
| Age, years | | | |
| > 64/≤ 64 | 0.964 | 0.342 to 2.717 | .9457 |
| EGFR mutation | | | |
| Mutant/wild-type | 0.342 | 0.117 to 0.998 | .0496 |

Abbreviation: EGFR, epidermal growth factor receptor.

Gefitinib sensitivity was essentially the same in COS cells transfected with L858R and in cells transfected with del L747-P753insS.[16] A more recent study showed that the tyrosine residue at codon 845 is highly phosphorylated in L858R mutants, but not in deletion mutants after epidermal growth factor binding.[23] This might explain the difference in gefitinib response between tumors with L858R and those with deletions.

Although our criteria for tumor response are soft, these are merely a surrogate marker for the effect on survival. We were able to show, for the first time, that *EGFR* mutation was the only significant and independent predictor for a prolonged survival after gefitinib treatment. In a previous study, we showed that *EGFR* mutation itself is not a predictor for better postoperative survival in 236 unselected patients with adenocarcinoma,[24] and in the present study, median disease-free interval was almost identical in patients with or without *EGFR* mutations. A recent placebo-controlled clinical trial showed that treatment with erlotinib, another oral EGFR TK inhibitor, significantly prolongs survival after first and second chemotherapy for NSCLC,[25] although *EGFR* mutation frequency is reported to be around 10% in Western countries.[15-17] This result is interpreted to mean that a subset of patients without mutations have also benefited from erlotinib therapy. The present study suggests that if patients were selected by presence of *EGFR* mutations, it would be possible to concentrate patients with benefits from gefitinib treatment, avoiding unnecessary adverse reactions such as fatal interstitial lung disease, which is relatively common in Japanese patients.[26] Furthermore, our results provide a basis for postoperative adjuvant gefitinib treatment in NSCLC patients with *EGFR* mutations, as adjuvant treatment is considered the earliest treatment of metastatic disease. These possibilities should be tested in future clinical trials.

It is common for patients to show progressive disease soon after presenting an initial striking response to

gefitinib. However, we could not detect any evidence that differences in classes of *EGFR* mutations are associated with duration of response (data not shown).

In conclusion, tumors with *EGFR* mutations showed good, but not perfect, correlation with clinical response in patients with postoperative recurrence of NSCLC. Furthermore, patients with *EGFR* mutations survived for a significantly longer period than those without *EGFR* mutations. Future clinical trials using gefitinib should examine *EGFR* mutations for effective selection of patients who are most likely to benefit from this molecular-targeted drug.


## Acknowledgment

We thank Kaori Hayashi-Hirano for excellent technical assistance in molecular analysis of tumors, and Ryuzo Ohno, President of Aichi Cancer Center, for special encouragement and support.


## Authors' Disclosures of Potential Conflicts of Interest

The following authors or their immediate family members have indicated a financial interest. No conflict exists for drugs or devices used in a study if they are not being evaluated as part of the investigation. Honoraria: Tetsuya Mitsudomi, AstraZeneca Japan, Bristol-Myers Squibb Japan, TAIHO Pharmaceutical. For a detailed description of this category, or for more information about ASCO's conflict of interest policy, please refer to the Author Disclosure Declaration and Disclosures of Potential Conflicts of Interest found in Information for Contributors in the front of each issue.

## REFERENCES


1. Kuroishi T, Hirose K, Tajima K: Cancer mortality in Japan, in Tominaga S, Oshima A (eds): Gann Monograph Cancer Research. Tokyo, Japan Scientific Societies Press, 1999, pp 1-38
2. Mitsudomi T, Viallet J, Linnoila RI, et al: Mutations of ras genes distinguish a subset of non-small cell lung cancer cell lines from small cell lung cancer cell lines. Oncogene 6:1353-1362, 1991
3. Mitsudomi T, Oyama T, Nishida K, et al: p53 nuclear immunostaining and gene mutations in non-small-cell lung cancer and their effects on patient survival. Ann Oncol 6:S9-13, 1995
4. Nishio M, Koshikawa T, Kuroishi T, et al: Prognostic significance of abnormal p53 accumulation in primary, resected non-small-cell lung cancers. J Clin Oncol 14:497-502, 1996
5. Nishio M, Koshikawa T, Yatabe Y, et al: Prognostic significance of cyclin D1 and Rb expression in combination with p53 abnormalities in primary, resected non-small cell lung cancer. Clin Cancer Res 3:1051-1058, 1997
6. Yatabe Y, Masuda A, Koshikawa T, et al: p27kip1 in human lung cancers: Differential changes in small cell and non-small cell carcinomas. Cancer Res 58:1042-1047, 1998
7. Hida T, Yatabe Y, Achiwa H, et al: Increased expression of cyclooxygenase 2 occurs frequently in human lung cancers, specifically in adenocarcinomas. Cancer Res 58:3761-3764, 1998
8. Arteaga CL: Overview of epidermal growth factor receptor biology and its role as a therapeutic target in human neoplasia. Semin Oncol 29:3-9, 2002
9. Bunn PA, Jr., Franklin W: Epidermal growth factor receptor expression, signal pathway, and inhibitors in non-small cell lung cancer. Semin Oncol 29:38-44, 2002
10. Ciardiello F, Tortora G: A novel approach in the treatment of cancer: Targeting the epidermal growth factor receptor. Clin Cancer Res 7:2958-2970, 2001
11. Kris MG, Natale RB, Herbst RS, et al: Efficacy of gefitinib, an inhibitor of the epidermal growth factor receptor tyrosine kinase, in symptomatic patients with non-small cell lung cancer: A randomized trial. JAMA 290:2149-2158, 2003
12. Fukuoka M, Yano S, Giaccone G, et al: Multi-institutional randomized phase II trial of gefitinib for previously treated patients with advanced non-small-cell lung cancer. J Clin Oncol 21:2237-2246, 2003
13. Cappuzzo F, Gregorc V, Rossi E, et al: Gefitinib in pretreated non-small-cell lung cancer (NSCLC): Analysis of efficacy and correlation with HER2 and epidermal growth factor receptor expression in locally advanced or metastatic NSCLC. J Clin Oncol 21:2658-2663, 2003
14. Suzuki T, Nakagawa T, Endo H, et al: The sensitivity of lung cancer cell lines to the EGFR-selective tyrosine kinase inhibitor ZD1839 ('Iressa') is not related to the expression of EGFR or HER-2 or to K-ras gene status. Lung Cancer 42:35-41, 2003
15. Paez JG, Janne PA, Lee JC, et al: EGFR mutations in lung cancer: Correlation with clinical response to gefitinib therapy. Science 304:1497-1500, 2004
16. Lynch TJ, Bell DW, Sordella R, et al: Activating mutations in the epidermal growth factor receptor underlying responsiveness of non-small-cell lung cancer to gefitinib. N Engl J Med 350:2129-2139, 2004
17. Pao W, Miller V, Zakowski M, et al: EGF receptor gene mutations are common in lung cancers from "never smokers" and are associated with sensitivity of tumors to gefitinib and erlotinib. Proc Natl Acad Sci U S A 101:13306-13311, 2004
18. Therasse P, Arbuck SG, Eisenhauer EA, et al: New guidelines to evaluate the response to treatment in solid tumors. European Organisation for Research and Treatment of Cancer, National Cancer Institute of the United States, National Cancer Institute of Canada. J Natl Cancer Inst 92:205-216, 2000
19. Salgia R, Harpole D, Herndon JE, 2nd, et al: Role of serum tumor markers CA 125 and CEA in non-small cell lung cancer. Anticancer Res 21:1241-1246, 2001
20. Mitsudomi T, Nishioka K, Maruyama R, et al: Kinetic analysis of recurrence and survival after potentially curative resection of nonsmall cell lung cancer. J Surg Oncol 63:159-165, 1996
21. Chemotherapy in non-small cell lung cancer: a meta-analysis using updated data on individual patients from 52 randomized trials. Non-Small Cell Lung Cancer Collaborative Group. BMJ 311:899-909, 1995
22. Yoshino I, Yohena T, Kitajima M, et al: Survival of non-small cell lung cancer patients with postoperative recurrence at distant organs. Ann Thorac Cardiovasc Surg 7:204-209, 2001
23. Sordella R, Bell DW, Haber DA, et al: Gefitinib-sensitizing EGFR mutations in lung cancer activate anti-apoptotic pathways. Science 305:1163-1167, 2004
24. Kosaka T, Yatabe Y, Endoh H, et al: Mutations of the epidermal growth factor receptor gene in lung cancer: Biological and clinical implications. Cancer Res 64:8919-8923, 2004
25. Shepherd FA, Pereira J, Ciuleanu TE, et al: A randomized placebo-controlled trial of erlotinib in patients with advanced non-small cell lung cancer following failure of 1st line or 2nd line chemotherapy. Proc Am Soc Clin Oncol 22:622s, 2004 (abstr 7022)
26. Inoue A, Saijo Y, Maemondo M, et al: Severe acute interstitial pneumonia and gefitinib. Lancet 361:137-139, 2003

# Reduced expression of *Dicer* associated with poor prognosis in lung cancer patients

Yoko Karube,[1,4] Hisaaki Tanaka,[1,5] Hirotaka Osada,[1] Shuta Tomida,[1] Yoshio Tatematsu,[1] Kiyoshi Yanagisawa,[1,5] Yasushi Yatabe,[2] Junichi Takamizawa,[1,5] Shinichiro Miyoshi,[4] Tetsuya Mitsudomi[3] and Takashi Takahashi[1,5,6]

[1]Division of Molecular Oncology, Aichi Cancer Center Research Institute; Departments of [2]Pathology and Molecular Diagnostics and [3]Thoracic Surgery Aichi Cancer Center Hospital, 1–1 Kanokoden, Chikusa-ku, Nagoya 464–0021; [4]Department of Cardio Thoracic Surgery, Dokkyo University School of Medicine, 880 Kitakobayashi, Mibu-machi, Shimotsuga-gun, Tochigi 321–0293; and [5]Division of Molecular Carcinogenesis, Center for Neural Disease and Cancer, Nagoya University School of Medicine, 65 Tsurumai-cho, Showa-ku, Nagoya 466–8550, Japan

(Received September 13, 2004/Revised November 24, 2004/Accepted Novermber 27, 2004/Online publication 17 February, 2005)

**Emerging evidence suggests that microRNA, which are well-conserved, abundant and small regulatory RNA, may be involved in the pathogenesis of human cancers. We recently reported that expression of *let-7* was frequently reduced in lung cancers, and that reduced *let-7* expression was significantly associated with shorter patient survival. Two members of the double-stranded RNA-specific endonuclease family, *Dicer* and *Drosha*, convert precursor forms of microRNA into their mature forms using a stepwise process. In the present study, we examined expression levels of these genes in 67 non-small cell lung cancer cases, and found for the first time that *Dicer* expression levels were reduced in a fraction of lung cancers with a significant prognostic impact on the survival of surgically treated cases. It should be noted that multivariate COX regression analysis showed that the prognostic impact of *Dicer* ($P = 0.001$) appears to be independent of disease stage ($P = 0.001$), while logistic regression analysis demonstrated that the higher incidence of reduced *Dicer* expression in poorly differentiated tumors remained significant even after correction for other parameters ($P = 0.02$). Given the fundamental and multiple biological roles of *Dicer* in various cellular processes, our results suggest the involvement of reduced *Dicer* expression in the development of lung cancers, thus warranting further investigations of the underlying mechanisms, which can be expected to enhance understanding of the molecular pathogenesis of this fatal cancer. (*Cancer Sci* 2005; 96: 111–115)**

## Introduction

Lung cancer is the leading cause of cancer-related death in Japan, as it is in many other economically developed countries.[1,2] The mutation, amplification and epigenetic changes of various genes, which may eliminate the normal function of gene products, have been identified in lung cancers, suggesting that they may be involved in pathogenesis.[3] In addition, emerging evidence suggests that microRNA, which constitute a well-conserved and abundant class of approximately 22-nucleotide regulatory RNA, could also be involved. We previously reported that the expression of *let-7* was frequently reduced in lung cancers, both *in vitro* and *in vivo*, and that reduced *let-7* expression was significantly associated with shorter patient survival.[4] Furthermore, we were able to demonstrate that over-expression of *let-7* resulted in significant inhibition of *in vitro* growth of lung cancer cells. In addition to our findings in lung cancers, a number of studies have dealt with microRNA alterations in other types of human cancers. These alterations include down-regulation of *miR15* and *miR16* in chronic lymphocytic leukemia as well as of *miR-143* and *miR-145* in human colon cancers.[5,6] The biological functions of microRNA are not yet fully understood, but it has been suggested that they play a role in the coordination of cell proliferation and cell death during development, in addition to their involvement in stress resistance.[7–9] This evidence appears to lend support to the notion that microRNA alterations could be involved in the genesis and/or progression of various human cancers.

A double-stranded RNA (dsRNA)-specific endonuclease converts precursor forms of microRNA into mature forms through a stepwise process, which includes the generation of ~70nt pre-microRNA with a characteristic hairpin structure from the longer nascent transcripts (pri-microRNA), and further processing into its mature form.[7–9] In humans, *Dicer* and *Drosha* are thought to collaborate in this stepwise processing of microRNA, with *Drosha* executing the initial step of microRNA processing in the nucleus,[10] and the resultant premicroRNA being exported to the cytoplasm where they are cleaved by *Dicer* to generate the final products of ~22nt.[11–16]

In this study, we posed a question as to whether expressions of *Dicer* and *Drosha*, which are essential for the processing of microRNA, are altered in lung cancers, and whether changes in the expression have any effect on clinicopathological features. To this end, we examined 67 non-small cell lung cancer (NSCLC) cases, which had undergone potentially curative surgical resection, by means of real-time RT-PCR. We report here for the first time that the reduced expression of *Dicer* in a significant fraction of lung cancers was associated with shorter postoperative survival.

## Materials and methods

**Patients and tumor sample preparations.** NSCLC samples were obtained from 67 patients who underwent potentially curative resection at the Aichi Cancer Center Hospital (Nagoya, Japan) between January 1996 and January 1998. Approval from the institutional review board and the patients' written informed consent were obtained. Stages were determined after pathologic evaluation of resected specimens according to the International System for Staging Lung Cancer, revised in 1997. The cohort consisted of 41 males and 26 females, with age at diagnosis ranging from 32 to 84 years (median age, 62 years). Thirty-seven patients had stage I disease, 13 patients stage II and 17 patients stage III. There were 15 patients with poorly differentiated, 43 with moderately and nine patients with well-differentiated tumors. Thirty-eight patients were smokers, and the remaining 29 had never smoked. A surgical pathologist (Y.Y.) performed a gross examination of the tissue specimens immediately after surgical removal, and pieces of tumor tissue were carefully selected for maximum tumor content. Half of each piece was snap frozen in liquid nitrogen, followed by storage at −80°C until use, and the other half was fixed with prechilled acetone and embedded in paraffin for confirmation of tumor contents. Total RNA was isolated by means of the standard acid

[6]To whom correspondence should be addressed. E-mail: tak@med.nagoya-u.ac.jp

 doi: 10.1111/j.1349-7006.2005.00015.x

guanidinium isothiocyanate/cesium chloride procedure using ultracentrifugation.

**Relative quantification by real-time RT-PCR analysis.** First-strand cDNA were synthesized from total RNA using Moloney murine leukemia virus reverse transcriptase (M-MLV RT) (Invitrogen, Carlsbad, CA, USA) and random hexamer primers (Roche Applied Science, Alameda, CA, USA). Real-time quantitative PCR amplification of a cDNA template corresponding to 20 ng total RNA was performed using SYBR Green Master Mix (Applied Biosystems, Foster City, CA, USA) in an ABI PRISM 7900-HT (Applied Biosystems). PCR conditions were 50°C for 2 min, 95°C for 10 min, followed by 55 cycles of 95°C for 30 s, 65°C for 30 s, and 72°C for 30 s. Standard curves were plotted by using serially diluted cDNA of the BEAS2B lung epithelial cell line, and the expression level of the samples was normalized with that of *18S rRNA* and expressed as a ratio of the normalized expression of the gene of interest in a mixture of the RNA of 38 normal lung tissues. Expression levels in this mixture of normal lung RNA were adopted as 1. The primer pairs used for *Dicer* were 5′-GTACGACTACCACAAGTACTTC-3′ and 5′-ATAGTACACCTGCCAGACTGT-3′, for *Drosha*, 5′-GTGC-TGTCCATGCACCAGATT-3′ and 5′-TGCATAACTCAACTGT-GCAGG-3′; and for *18S rRNA*, 5′-AATCAGGGTTCGATTCCGGA-3′ and 5′-CCAAGATCCAACTACGAGCT-3′.

**DNA methylation analysis of *Dicer*.** Extraction of genomic DNA from tissues was performed according to standard procedures. Genomic DNA were treated with the bisulfite conversion method as described in a previous study.[17] After conversion, the promoter region of *Dicer* was amplified by PCR and every CpG site within the region was examined with direct sequencing for the presence of DNA methylation. The primer sequence was designed on the basis of the converted sense strand sequences without CpG sites 5′-TTTATTTGGGTTTGTAGTAGT-3′ and 5′-AACCCTATCCAATCACAAACT-3′. The PCR mixture contained 1 unit of Platinum Taq DNA polymerase (Invitrogen) together with 1 × PCR buffer, 2.5 m*M* of $MgCl_2$, 25 pmol of each primer, and 0.2 m*M* of dNTP. PCR conditions were 95°C for 5 min, followed by 40 cycles at 95°C for 30 s, at 56°C for 30 s, at 72°C for 45 s, and at 72°C for 5 min. The PCR products were gel extracted (QIAquick Gel Extraction Kit; Qiagen, Valencia, CA, USA) and sequenced directly with the aid of an ABI PRISM BigDye Terminator Cycle Sequencing Kit (Applied Biosystems).

**Statistical analysis.** The following biostatistical analyses were performed with the STATA statistical package release 7.0 (STATA, College Station, TX, USA). The $\chi^2$ goodness-of-fit test was used to analyze whether the distribution of expression levels at $\log_2$ of *Dicer* or *Drosha* could be fitted to the normal distribution. Student's *t*-test was employed to determine the best cut-off value for separating two characteristic groups in terms of gene expression levels. The association between expression levels of *Dicer* and *Drosha* was analyzed by computing the Pearson correlation coefficient, and associations between various clinicopathologic characteristics and the expression levels of *Dicer* and *Drosha* were examined by means of Fisher's exact test. The Kaplan-Meier estimates of overall survival time were compared by using the log-rank test. Cox regression analysis of factors potentially related to survival was used to identify which independent factors might jointly have a significant effect on survival. All tests were two-tailed, and the significance level was set at $P < 0.05$.

## Results

**Reduced expression of *Dicer* in NSCLC.** We used real-time RT-PCR analysis to examine 67 NSCLC cases, which had undergone potentially curative resection, for *Dicer* and *Drosha* expression. We found that there was a significant correlation between *Dicer* and *Drosha* expression in NSCLC, with a Pearson correlation coefficient of 0.79 ($P < 0.001$; Fig. 1a).

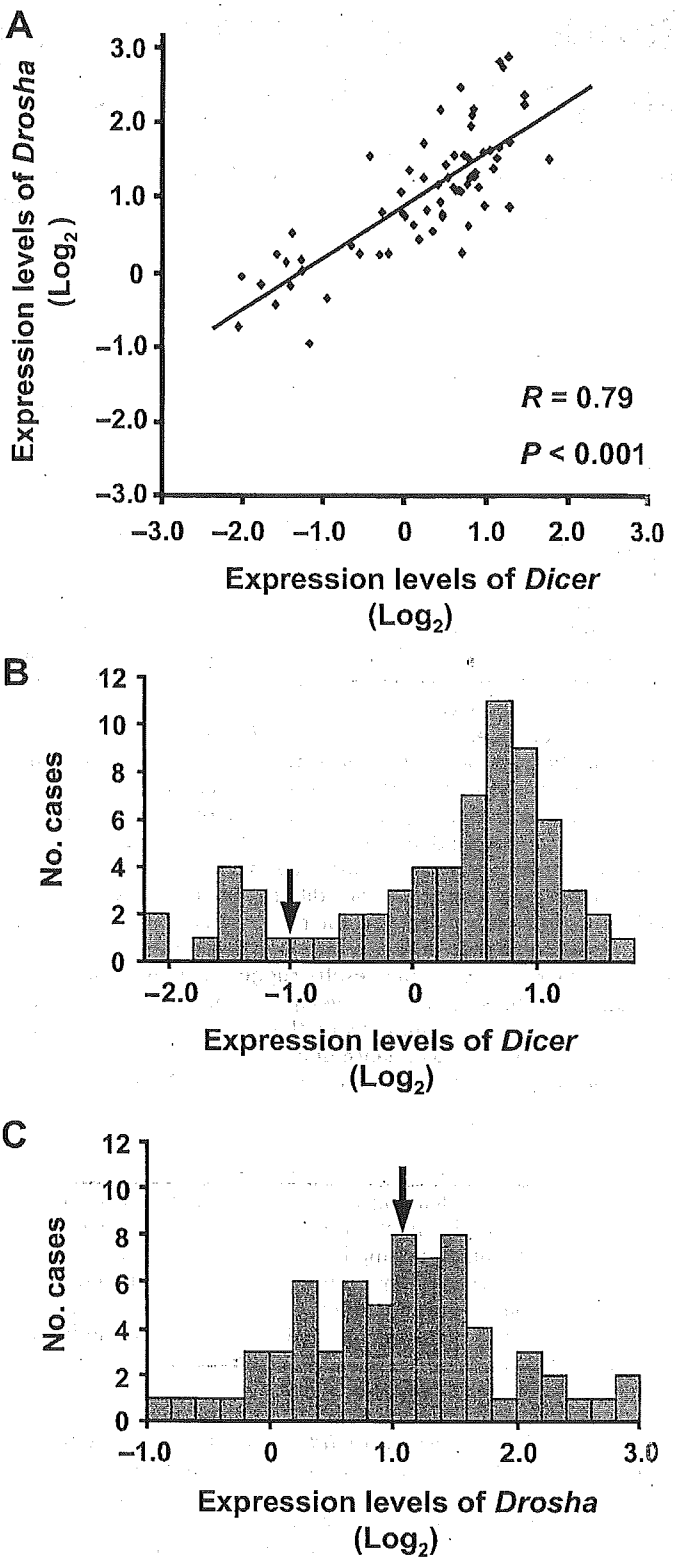


**Fig. 1.** Histograms of distributions of non-small cell lung cancers (NSCLC) according to their expression of double-stranded RNA-specific endonucleases mRNA. (A) Scattered plot analysis of expression levels of *Dicer* and *Drosha*. (B) Histogram of *Dicer* expression level at $\log_2$ value in NSCLC. With the threshold set at −1.0 of $\log_2$ value, patients were divided into two groups: low, with *Dicer* $\log_2$ value expression <−1.0; and high, with *Dicer* $\log_2$ value expression = −1.0. (C) Histogram of *Drosha* $\log_2$ value expression level in NSCLC. With the threshold set at 1.1 of $\log_2$ value, patients were divided into two groups: low, with *Drosha* $\log_2$ value expression <1.1; and high, with *Dicer* $\log_2$ value expression = 1.1. X-axis, $\log_2$ value; Y-axis, number of cases.



 doi: 10.1111/j.1349-7006.2005.00015.x

Table 1. Relationship between expression levels of *Dicer* and *Drosha* and various clinicopathologic characteristics

| Characteristics | No. cases | *Dicer* | | | *Drosha* | | |
|---|---|---|---|---|---|---|---|
| | | High | Low | *P** | High | Low | *P** |
| Age (years) | | | | | | | |
| ≤62 | 34 | 29 | 5 | 0.75 | 22 | 12 | 0.03 |
| >62 | 33 | 27 | 6 | | 12 | 21 | |
| Sex | | | | | | | |
| Male | 41 | 34 | 7 | 1.00 | 21 | 20 | 1.00 |
| Female | 26 | 22 | 4 | | 13 | 13 | |
| Histology | | | | | | | |
| Squamous | 11 | 10 | 1 | 0.68 | 5 | 6 | 0.75 |
| Non-squamous | 56 | 46 | 10 | | 29 | 27 | |
| Smoking history | | | | | | | |
| Smoker | 38 | 31 | 7 | 0.75 | 19 | 19 | 1.00 |
| Non-smoker | 29 | 25 | 4 | | 15 | 14 | |
| Disease stage | | | | | | | |
| I | 37 | 31 | 6 | 1.00 | 20 | 17 | 0.63 |
| II-III | 30 | 25 | 5 | | 14 | 16 | |
| Differentiation | | | | | | | |
| Poor | 15 | 9 | 6 | 0.01 | 5 | 10 | 0.15 |
| Well or moderate | 52 | 47 | 5 | | 29 | 23 | |

*Two-sided Fisher's exact test.

However, close inspection of the distributions of their expression disclosed a clear difference. A histogram of the expression of *Dicer* showed a frequency distribution with two prominent peaks at $\log_2$ values from −1.6 to −1.4 and from 0.6 to 0.8 (Fig. 1B), which was in marked contrast to that of *Drosha* (Fig. 1C). We used the $\chi^2$ goodness-of-fit test to determine whether the observed frequency distributions of expression of *Dicer* and *Drosha* could be fitted to the normal distribution. In the case of *Dicer*, it was clear that the data were not normally distributed ($P < 0.001$). The Student's *t*-test was therefore used to identify the cut-off value with the highest potential for discriminating two distinct groups in terms of *Dicer* expression. Patients could be divided most clearly and consistently into two groups with low and high expression of *Dicer* when the distribution threshold was set at −1.0 of the $\log_2$ ratio of *Dicer* expression. In contrast to the findings for *Dicer*, the hypothesis that the distribution of *Drosha* follows a normal distribution pattern could not be rejected ($P = 0.97$). Accordingly, the median expression level (i.e. 1.1 of the $\log_2$ value) was chosen as the threshold value to be used for further analysis.

**Relationships between expression of *Dicer* and *Drosha* and various clinicopathologic characteristics.** Our next investigation was concerned with whether expression levels of either *Dicer* or *Drosha* showed any relationship with the clinicopathologic characteristics of lung cancers, and found that there was a statistically significant association between *Dicer* expression levels and differentiation grade (Table 1). Cases with low *Dicer* expression showed significantly greater prevalence of poorly differentiated tumors than those with high *Dicer* expression ($P = 0.01$), which was also observed in the multivariate logistic regression analysis with adjustment for all the variables analyzed in the univariate analysis ($P = 0.02$).

**Association between low *Dicer* expression and shortened postoperative survival.** The next question to be examined was whether expression levels of *Dicer* and *Drosha* were associated with patient survival after surgery. The Kaplan-Meier survival curves demonstrated that the probability of survival was significantly lower for the group of patients with low levels of *Dicer* expression ($P = 0.0001$ by log-rank test; Fig. 2A), while low expression of *Drosha* tended to be associated with a worse prognosis ($P = 0.06$ by log-rank test; Fig. 2B). Prognostic values of various factors were studied by univariate Cox regression

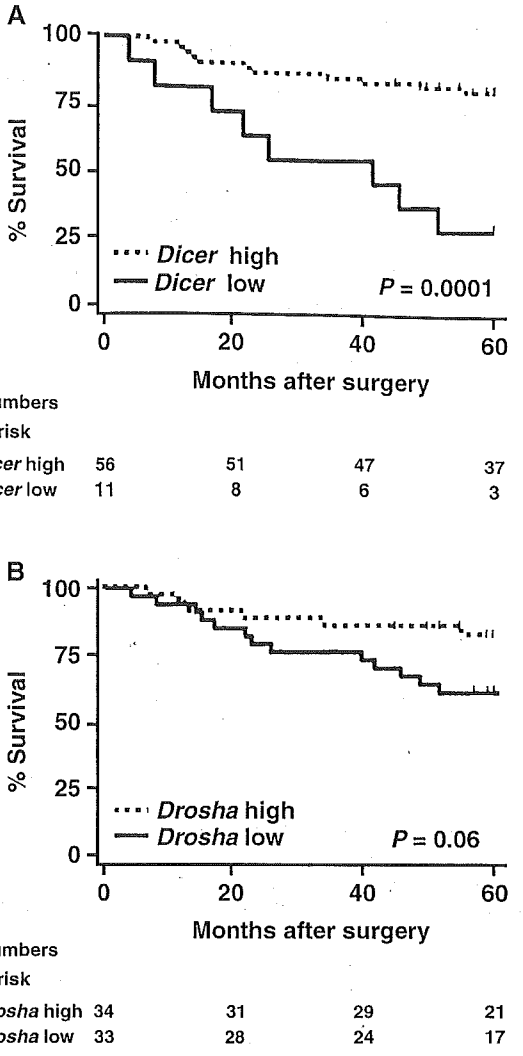


**Fig. 2.** Analysis of overall survival of patients with high or low expression of double-stranded RNA-specific endonucleases. (A) Kaplan-Meier survival curves for lung cancer patients, who were classified as showing either high or low *Dicer* expression. *Dicer* status was found to be strongly associated (log-rank, $P = 0.0001$) with patient survival. (B) Kaplan-Meier survival curve for lung cancer patients, who were classified as showing either high or low *Drosha* expression. *Drosha* status did not show a significant (log-rank, $P = 0.06$) relationship with patient survival. X-axis, length of survival after surgery; Y-axis, percentage of survivors.

analysis (Table 2). It was shown that, in addition to disease stage ($P = 0.003$), low *Dicer* expression was a significant predictive factor for poor prognosis ($P < 0.001$), whereas the *Drosha* expression level did not show a significant association with survival ($P = 0.07$).

The interrelationship of possible prognostic factors and survival was further analyzed by means of the Cox proportional hazards modeling using age, sex, histology, smoking history, disease stage and differentiation as well as expression levels of *Dicer* and *Drosha* as variables. As a result, reduced expression of *Dicer*, in addition to disease stage ($P = 0.001$), was identified as a significant and independent prognostic factor ($P = 0.001$) for surgically treated NSCLC patients after potentially curative resection. The hazard ratio for earlier death was 17.6 [95% confidence interval: 3.49–89.1] for low versus high expression levels of *Dicer*. These findings provided a strong indication that the expression levels of *Dicer* appeared to have a significant impact on the postoperative survival of NSCLC patients.

Table 2. Univariate and multivariate Cox regression analyses of the relationship between expression levels of *Dicer* and various clinical characteristics

Univariate analysis

| Variables | HR [95% CI] | Unfavorable/Favorable | *P* |
|---|---|---|---|
| Age (years) | 2.02 [0.80–5.14] | >62/≤62 | 0.14 |
| Sex | 2.79 [0.92–8.41] | Male/Female | 0.07 |
| Histology | 1.37 [0.45–4.14] | Squamous/Non-squamous | 0.58 |
| Smoking history | 2.52 [0.91–7.01] | Smoker/Non-smoker | 0.08 |
| Disease stage | 4.61 [1.66–12.85] | II-III/I | 0.003 |
| Differentiation | 2.55 [1.00–6.49] | Poor/Well or moderate | 0.05 |
| *Dicer* | 5.18 [2.07–12.97] | Low/High | <0.001 |
| *Drosha* | 2.45 [0.93–6.45] | Low/High | 0.07 |

Multivariate analysis

| Variables | HR [95% CI] | Unfavorable/Favorable | *P* |
|---|---|---|---|
| Age (years) | 1.86 [0.64–5.43] | >62/≤62 | 0.26 |
| Sex | 1.08 [0.25–4.64] | Male/Female | 0.92 |
| Histology | 1.14 [0.29–4.51] | Squamous/Non-squamous | 0.85 |
| Smoking history | 2.89 [0.75–11.1] | Smoker/Non-smoker | 0.12 |
| Disease stage | 11.3 [2.87–44.3] | II-III/I | 0.001 |
| Differentiation | 0.48 [0.12–1.86] | Poor/Well or moderate | 0.29 |
| *Dicer* | 17.6 [3.49–89.1] | Low/High | 0.001 |
| *Drosha* | 0.91 [0.25–3.36] | Low/High | 0.88 |

HR, hazard ratio; CI, confidence interval.

**Lack of DNA methylation of the *Dicer* promoter region.** Because DNA methylation of the promoter region is thought to be significantly involved in transcriptional regulation,[18] we used the bisulfite conversion technique to study DNA methylation of the *Dicer* promoter region in 15 NSCLC (10 with low *Dicer* expression and five with high *Dicer* expression), as well as in three normal lung tissues. No methylation of the *Dicer* promoter region was found in any of the cases regardless of the level of *Dicer* expression, thus suggesting the involvement of other underlying mechanisms in the reduction of *Dicer* expression.

## Discussion

In the study presented here, we have shown that the reduced expression of *Dicer* in a significant fraction of lung cancers is associated with shorter postoperative survival. To the best of our knowledge, ours is the first report of alterations of *Dicer* in human cancers. It should be noted that among the variables used in the multivariate COX regression analysis (i.e. age, sex, histology, smoking history, disease stage and differentiation as well as expression levels of *Dicer* and *Drosha*), *Dicer* appears to have a significant prognostic impact ($P = 0.001$) independent of disease stage ($P = 0.001$). Because logistic regression analysis demonstrated that the higher incidence of reduced *Dicer* expression in poorly differentiated tumors remained significant even after correction for other parameters ($P = 0.02$), one can speculate that prognostic impact of poor differentiation may well be represented by the presence of reduced expression of *Dicer*. Although our finding needs to be confirmed, for example on the cutoff value of *Dicer* expression level, by a further validation study using an independent and larger cohort, reduced expression of *Dicer* appears to be clinically useful for the prognosis of lung cancer patients. As for the underlying mechanisms involved in reduced *Dicer* expression in lung cancers, our study suggests that the involvement of hypermethylation of CpG sites in the promoter region is unlikely, so that other possibilities such as altered chromatin conformation and haploinsufficiency need to be pursued.[18] Corresponding to this, the frequent occurrence of loss of heterozygosity (LOH) on the long arm of chromosome 14, where *Dicer* resides, has been reported in lung cancers,[19,20] while a number of studies have also indicated that this chromosomal region is often affected in various other human cancers.[21–26] It is interesting that LOH on 14q appears to be related to tumor progression of colon cancer, with a higher incidence of this anomaly in metastatic sites than in primary tumors.[27]

Accumulating evidence supports the notion that the prognostic impact of reduced *Dicer* expression observed in our study might have a functional role in the development of lung cancers rather than being a mere surrogate marker. In correspondence with this, we recently reported that expression levels of *let-7* microRNA were frequently reduced in lung cancers, both *in vitro* and *in vivo*, and that lung cancer patients with reduced *let-7* expression had a significantly worse prognosis after potentially curative resection independent of disease stage.[4] We note that significant associations between reduced expression of *Dicer* and those of *let-7a-1* ($R = 0.66$, $P < 0.001$) and *let-7f-1* ($R = 0.65$, $P < 0.001$) were observed in this study. Since *Dicer* is required in the processing and generation of a fully mature form of microRNA,[11–16] it is not inconceivable that reduced *Dicer* expression may constitute an alternate post-transcriptional mechanism, which can also reduce expression levels of *let-7* and probably other microRNA in cancer cells.

In addition, other factors may underlie the potential biological effects of reduced *Dicer* expression in lung cancer cells. In fact, accumulating evidence suggests that the RNAi machinery may be functionally linked to the regulation of chromosome dynamics and genomic integrity. Furthermore, eukaryotic heterochromatin is characterized by a high density of repeats as well as by modified histones, and influences both gene expression and chromosome segregation. It was also found that deletion of *Dicer* in the fission yeast *Schizosaccharomyces pombe* resulted in the aberrant accumulation of complementary transcripts from centromeric heterochromatic repeats, loss of histone H3 lysine-9 methylation, and impairment of centromere function, resulting in defects in proper chromosome segregation.[28–32] The presence of marked aneuploidy is one of the key features of lung cancers,[33] while we previously reported the presence of a persistent increase in the rate of chromosomal losses and gains (i.e. chromosome instability, or CIN),[34] as well as of frequent impairment of mitotic checkpoints in lung cancer cell lines.[35] Therefore, the results of the present study raise the possibility that reduced *Dicer* expression in lung cancers may render cancer cells susceptible to chromosomal missegregation, in part because of the dysfunction of centromeres in the absence of a surveillance mechanism, which is the impairment of mitotic checkpoints.

It has also been suggested that the RNAi machinery might be involved in X inactivation and imprinting through sequence-specific histone modification and consequential DNA methylation and epigenetic silencing.[28] Therefore, it is possible that reduced expression of *Dicer* may affect such transcriptional regulation, resulting from the altered activity of the RNAi machinery. In this connection, it should be noted that we previously found that loss of genomic imprinting is a frequent event in human lung cancers.[36,37] It would therefore be of considerable interest to study the involvement of a reduction in *Dicer* expression in relation to altered genomic imprinting in lung cancers.

In conclusion, we have been able to demonstrate for the first time that *Dicer* expression levels are reduced in some lung cancers with a significant prognostic impact on the survival of surgically treated cases. Given the fundamental and multiple biological roles of *Dicer* in various cellular processes, our results suggest the involvement of reduced *Dicer* expression in the development of lung cancers, and clearly warrant further investigations of the underlying mechanisms by which this alteration affects patient prognosis for a better understanding of the molecular pathogenesis of this fatal cancer. In addition, future studies to investigate


 doi: 10.1111/j.1349-7006.2005.00015.x

whether altered *Dicer* expression is present in other types of human cancers should be both interesting and important.

## Acknowledgments

The authors would like to thank Dr Keitaro Matuo at Division of Epidemiology and Prevention of Aichi Cancer Center for his helpful suggestions in biostatistical analysis. This work was supported in part by a Grant-in-Aid for Scientific Research on Priority Areas from the Ministry of Education, Culture, Sports, Science and Technology of Japan, a Grant-in-Aid for Scientific Research (B) from the Japan Society for the Promotion of Science and a Grant-in-Aid for the Second Term Comprehensive Ten-Year Strategy for Cancer Control from the Ministry of Health and Welfare, Japan.

## References

1 Minna JD. Neoplasms of the lung. In: Fauci A, Braunwald E, Kasper D, Hauser S, Longo D, Jameson J (eds). *Harrison's principles of internal medicine*, 15th edn. McGraw-Hill, New York 2001; 562–71.
2 Statistics and Information Department, Minister's Secretariat. *Vital statistics of Japan 2001*, Vol. 3. Ministry of Health, Labor and Welfare, Tokyo 2003; 384–411.
3 Osada H, Takahashi T. Genetic alterations of multiple tumor suppressors and oncogenes in the carcinogenesis and progression of lung cancer. *Oncogene* 2002; **21**: 7421–34.
4 Takamizawa J, Konishi H, Yanagisawa K, Tomida S, Osada H, Endoh H, Harano T, Yatabe Y, Nagino M, Nimura Y, Mitsudomi T, Takahashi T. Reduced expression of the let-7 microRNA in human lung cancers in association with shortened postoperative survival. *Cancer Res* 2004; **64**: 3753–6.
5 Calin GA, Dumitru CD, Shimizu M, Bichi R, Zupo S, Noch E, Aldler H, Rattan S, Keating M, Rai K, Rassenti L, Kipps T, Negrini M, Bullrich F, Croce CM. Frequent deletions and down-regulation of micro-RNA genes miR15 and miR16 at 13q14 in chronic lymphocytic leukemia. *Proc Natl Acad Sci U S A* 2002; **99**: 15524–9.
6 Michael MZ, Sm OC, van Holst Pellekaan NG, Young GP, James RJ. Reduced accumulation of specific microRNA in colorectal neoplasia. *Mol Cancer Res* 2003; **1**: 882–91.
7 Ambros V. MicroRNA pathways in flies and worms. growth, death, fat, stress, and timing. *Cell* 2003; **113**: 673–6.
8 Bartel DP. MicroRNA: genomics, biogenesis mechanism and function. *Cell* 2004; **116**: 281–97.
9 Grosshans H, Slack FJ. Micro-RNA: small is plentiful. *J Cell Biol* 2002; **156**: 17–21.
10 Lee Y, Ahn C, Han J, Choi H, Kim J, Yim J, Lee J, Provost P, Radmark O, Kim S, Kim VN. The nuclear RNase III Drosha initiates microRNA processing. *Nature* 2003; **425**: 415–9.
11 Hutvagner G, McLachlan J, Pasquinelli AE, Balint E, Tuschl T, Zamore PD. A cellular function for the RNA-interference enzyme Dicer in the maturation of the let-7 small temporal RNA. *Science* 2001; **293**: 834–8.
12 Bernstein E, Caudy AA, Hammond SM, Hannon GJ. Role for a bidentate ribonuclease in the initiation step of RNA interference. *Nature* 2001; **409**: 363–6.
13 Grishok A, Pasquinelli AE, Conte D, Li N, Parrish S, Ha I, Baillie DL, Fire A, Ruvkun G, Mello CC. Genes and mechanisms related to RNA interference regulate expression of the small temporal RNA that control *C. elegans* developmental timing. *Cell* 2001; **106**: 23–34.
14 Ketting RF, Fischer SE, Bernstein E, Sijen T, Hannon GJ, Plasterk RH. Dicer functions in RNA interference and in synthesis of small RNA involved in developmental timing in *C. elegans*. *Genes Dev* 2001; **15**: 2654–9.
15 Knight SW, Bass BL. A role for the RNase III enzyme DCR-1 in RNA interference and germ line development in *Caenorhabditis elegans*. *Science* 2001; **293**: 2269–71.
16 Lee Y, Jeon K, Lee JT, Kim S, Kim VN. MicroRNA maturation: stepwise processing and subcellular localization. *Embo J* 2002; **21**: 4663–70.
17 Osada H, Tatematsu Y, Masuda A, Saito T, Sugiyama M, Yanagisawa K, Takahashi T. Heterogeneous transforming growth factor (TGF)-β unresponsiveness and loss of TGF-β receptor type II expression caused by histone deacetylation in lung cancer cell lines. *Cancer Res* 2001; **61**: 8331–9.
18 Bird A. DNA methylation patterns and epigenetic memory. *Genes Dev* 2002; **16**: 6–21.
19 Abujiang P, Mori TJ, Takahashi T, Tanaka F, Kasyu I, Hitomi S, Hiai H. Loss of heterozygosity (LOH) at 17q and 14q in human lung cancers. *Oncogene* 1998; **17**: 3029–33.
20 Wong MP, Lam WK, Wang E, Chiu SW, Lam CL, Chung LP. Primary adenocarcinomas of the lung in nonsmokers show a distinct pattern of allelic imbalance. *Cancer Res* 2002; **62**: 4464–8.
21 Suzuki T, Yokota J, Mugishima H, Okabe I, Ookuni M, Sugimura T, Terada M. Frequent loss of heterozygosity on chromosome 14q in neuroblastoma. *Cancer Res* 1989; **49**: 1095–8.
22 Cliby W, Ritland S, Hartmann L, Dodson M, Halling KC, Keeney G, Podratz KC, Jenkins RB. Human epithelial ovarian cancer allelotype. *Cancer Res* 1993; **53**: 2393–8.
23 Nawroz H, van der Riet P, Hruban RH, Koch W, Ruppert JM, Sidransky D. Allelotype of head and neck squamous cell carcinoma. *Cancer Res* 1994; **54**: 1152–5.
24 Chang WY, Cairns P, Schoenberg MP, Polascik TJ, Sidransky D. Novel suppressor loci on chromosome 14q in primary bladder cancer. *Cancer Res* 1995; **55**: 3246–9.
25 Herbers J, Schullerus D, Muller H, Kenck C, Chudek J, Weimer J, Bugert P, Kovacs G. Significance of chromosome arm 14q loss in nonpapillary renal cell carcinomas. *Genes Chromosomes Cancer* 1997; **19**: 29–35.
26 De Rienzo A, Jhanwar SC, Testa JR. Loss of heterozygosity analysis of 13q and 14q in human malignant mesothelioma. *Genes Chromosomes Cancer* 2000; **28**: 337–41.
27 Young J, Leggett B, Ward M, Thomas L, Buttenshaw R, Searle J, Chenevix-Trench G. Frequent loss of heterozygosity on chromosome 14 occurs in advanced colorectal carcinomas. *Oncogene* 1993; **8**: 671–5.
28 Volpe TA, Kidner C, Hall IM, Teng G, Grewal SI, Martienssen RA. Regulation of heterochromatic silencing and histone H3 lysine-9 methylation by RNAi. *Science* 2002; **297**: 1833–7.
29 Hall IM, Shankaranarayana GD, Noma K, Ayoub N, Cohen A, Grewal SI. Establishment and maintenance of a heterochromatin domain. *Science* 2002; **297**: 2232–7.
30 Provost P, Silverstein RA, Dishart D, Walfridsson J, Djupedal I, Kniola B, Wright A, Samuelsson B, Radmark O, Ekwall K. Dicer is required for chromosome segregation and gene silencing in fission yeast cells. *Proc Natl Acad Sci U S A* 2002; **99**: 16648–53.
31 Hall IM, Noma K, Grewal SI. RNA interference machinery regulates chromosome dynamics during mitosis and meiosis in fission yeast. *Proc Natl Acad Sci U S A* 2003; **100**: 193–8.
32 Volpe T, Schramke V, Hamilton GL, White SA, Teng G, Martienssen RA, Allshire RC. RNA interference is required for normal centromere function in fission yeast. *Chromosome Res* 2003; **11**: 137–46.
33 Masuda A, Takahashi T. Chromosome instability in human lung cancers: possible underlying mechanisms and potential consequences in the pathogenesis. *Oncogene* 2002; **21**: 6884–97.
34 Haruki N, Harano T, Masuda A, Kiyono T, Takahashi T, Tatematsu Y, Shimizu S, Mitsudomi T, Konishi H, Osada H, Fujii Y, Takahashi T. Persistent increase in chromosome instability in lung cancer: possible indirect involvement of p53 inactivation. *Am J Pathol* 2001; **159**: 1345–52.
35 Takahashi T, Haruki N, Nomoto S, Masuda A, Saji S, Osada H, Takahashi T. Identification of frequent impairment of the mitotic checkpoint and molecular analysis of the mitotic checkpoint genes, hsMAD2 and p55CDC, in human lung cancers. *Oncogene* 1999; **18**: 4295–300.
36 Suzuki H, Ueda R, Takahashi T. Altered imprinting in lung cancer. *Nat Genet* 1994; **6**: 332–3.
37 Kondo M, Suzuki H, Ueda R, Osada H, Takagi K, Takahashi T, Takahashi T. Frequent loss of imprinting of the H19 gene is often associated with its overexpression in human lung cancers. *Oncogene* 1995; **10**: 1193–8.

Lung Cancer (2005) 47, 235–242

ELSEVIER

LUNG CANCER

IASLC

www.elsevier.com/locate/lungcan

# Pitfalls in lymph node staging with positron emission tomography in non-small cell lung cancer patients

Kazuya Takamochi[a,b,*], Junji Yoshida[a], Koji Murakami[d], Seiji Niho[a], Genichiro Ishii[c], Mitsuyo Nishimura[a], Yutaka Nishiwaki[a], Kazuya Suzuki[b], Kanji Nagai[a]

[a] *Department of Thoracic Oncology, National Cancer Center Hospital East, Chiba, Japan*
[b] *First Department of Surgery, Hamamatsu University School of Medicine 1-20-1 Handayama, Hamamatsu, Shizuoka 431-3192, Japan*
[c] *Pathology Division, National Cancer Center Research Institute East, Chiba, Japan*
[d] *Department of Radiology, National Cancer Center Hospital East, Chiba, Japan*

Received 3 March 2004; received in revised form 3 August 2004; accepted 18 August 2004

KEYWORDS
Non-small cell lung cancer;
Positron emission tomography;
Diagnosis;
Staging;
False-positive;
False-negative

**Summary**
*Background:* The evidence of clinical value of positron emission tomography (PET) with fluorine-18 fluorodeoxyglucose (FDG) in lymph node (LN) staging in non-small cell lung cancer (NSCLC) has been shown in numerous papers. However, few studies have assessed its limitations. The aim of the present study is to clarify clinicopathologic factors responsible for false PET results.
*Methods:* From July 2000 through December 2001, 71 NSCLC patients underwent both FDG PET and surgical intervention at the National Cancer Center Hospital East, Chiba. Clinical records, computed tomographic (CT) scan findings, PET findings, and histologic findings were retrospectively reviewed.
*Results:* Sensitivity, specificity, accuracy in nodal staging for CT were 29, 83, and 65% and for PET were 39, 79, and 66%, respectively. There were 10 (14%) false-positive PET scans and 14 (20%) false-negative PET scans. The causative factors for false-positive PET scan were: (1) inflammatory conditions in seven patients; (2) PET mis-localization of an interlobar LN as a mediastinal LN in one patient; (3) inability to distinguish the endobronchial polypoid growth of a primary tumor from a lobar LN in one patient; (4) unknown in one patient. All false-positive LNs due to inflammatory conditions showed reactive lymphoid hyperplasia histologically. The causative factors for false-negative PET scan were: (1) limitation of spatial resolution

* Corresponding author. Tel.: +81 53 435 2276; fax: +81 53 435 2272.
*E-mail address:* ktakamoc@hama-med.ac.jp (K. Takamochi).


doi:10.1016/j.lungcan.2004.08.004

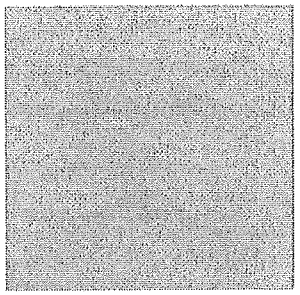

of the PET scanner in 12 patients (maximum tumor focus dimensions in false-negative LNs ranging from 1 to 7.5 mm, with an average of 3.4 mm); (2) PET mis-localization of a mediastinal LN as a hilar LN in one patient; (3) weak FDG uptake by microscopic tumor foci due to necrosis with massive bleeding in a metastatic LN in one patient. **Conclusions:** Inflammatory conditions were most responsible for false-positive PET scans, and spatial resolution limitation of FDG PET was the causative factor of false-negative PET scans. Recognizing these factors in advance would be clinically helpful in accurate nodal staging with FDG PET.


## 1. Introduction

Accurate lymph node (LN) staging is critical in determining treatment strategy and predicting outcome for patients with non-small cell lung cancer (NSCLC). Patients without metastatic LN (N0) or with only intrapulmonary or hilar LN involvement (N1) are candidates for straightforward surgical resection. Patients with ipsilateral metastatic mediastinal LN (N2) are usually treated with chemo-radiotherapy or with induction therapy followed by surgery. Patients with further node involvement (N3) are not considered for primary surgery, and chemo-radiotherapy is indicated.

Computed tomographic (CT) scanning is the most widely accepted non-invasive imaging modality for nodal staging in NSCLC patients, but it is far from satisfying and is less accurate than invasive surgical staging such as mediastinoscopy, mediastinotomy, or video-assisted thoracoscopic surgery [1,2]. CT is an anatomic imaging tool that demonstrates LN enlargement as a sign of metastasis. It is generally agreed that normal-sized LNs can harbour metastases while enlarged LNs can be metastasis-free [3–6]. It is not possible to accurately diagnose LN status based on CT measurement alone.

By contrast, positron emission tomography (PET) with fluorine-18 fluorodeoxyglucose (FDG) provides functional images of glucose uptake and phosphorylation [7]. Meta-analytic studies [8–11] have demonstrated that PET was significantly more accurate than CT for nodal staging in NSCLC. Although FDG PET represents an important advance in NSCLC nodal staging, there are some false-positive and false-negative results in any studies. Thus, invasive surgical staging still remains the gold standard for accurate nodal staging.

To date, few studies have attempted to determine the causative factors of false PET results in nodal staging in NSCLC [12–14]. Recognizing these factors in advance would be clinically helpful in accurate nodal staging with FDG PET. The aim of this study is to clarify clinico-pathologic factors responsible for false PET results.

## 2. Materials and methods

### 2.1. Patients

From July 2000 through December 2001, FDG PET was performed in 226 patients with thoracic abnormalities at the National Cancer Center Hospital East. Among them, we retrospectively reviewed 71 patients with proven or suspected NSCLC, who later had pathologic confirmation of their resected tumor and nodal status, in this study. These patients underwent PET to evaluate their indeterminate lung lesions or to determine the preoperative staging. Patients with obvious bulky mediastinal lymph adenopathy were excluded. Not all surgical candidates during the same period were included, because of limited PET examination capacity at our institute. Informed consent for FDG PET was obtained from all patients.

There were 41 men and 30 women, and their ages ranged from 36 to 90 years (median 65 years). Seventy of the 71 patients underwent major lung resection and systematic lymph node dissection. The remaining one patient underwent preoperative mediastinoscopy, which revealed mediastinal node involvement, and received combined chemoradiotherapy. No patient in this study had received induction therapy. CT, PET and surgery were carried out within 1 month in all patients.

### 2.2. FDG PET

All patients were asked to keep fasting for at least 6 h before FDG injection in order to minimize the blood insulin level and normal tissue glucose uptake. Serum glucose levels before FDG injection were 150 mg/dl or lower in all patients. Whole body FDG PET imaging was performed using a GE Advance Scanner (General Electric Medical System, Milwaukee, WI), which has an axial field of view of 15 cm and a spatial resolution of 4.5 mm full-width-half-maximum. PET imaging included the entire field of view from the skull base to the thigh. Sixty min-

utes after intravenous injection of 300 MBq of F-18 FDG, emission scanning was performed in 5 min, and transmission scanning in 1 min. Data acquisition was performed in seven bed positions.

All PET images were interpreted by one or two experienced nuclear medicine radiologists. The 4.25 mm-thick images were reviewed in axial, coronal, and sagittal planes on hard copy films. Based on a visual comparison between CT and PET, LN stations of abnormal uptake were determined according to Naruke's lymph node mapping [15]. LNs were considered positive for malignancy when uptake was greater than the mediastinal blood pool activity by visual estimation.

### 2.3. Thoracic CT

CT was performed before PET imaging in all patients. CT was done with an X-Vigor or an Aquilion (Toshiba Medical Systems, Tokyo, Japan), and contiguous 5—7.5 mm thick sections were obtained from the pulmonary apices to the bases in a supine position at full inspiration. Dynamic incremental scanning was always performed, after bolus injection of 100 ml of contrast material using an automatic injector.

All contrast-enhanced CT films were interpreted by at least two experienced thoracic radiologists. The following findings were recorded: the maximum dimension and location of the primary lesion, LN sizes, obstructive pneumonia or atelectasis owing to primary tumor, and pulmonary fibrosis. The location of a primary tumor was defined to be central when it was located in the inner one third of the lung field, and peripheral when in the outer two thirds on CT scan. LNs larger than 1 cm in the shortest dimension were considered positive for malignancy. LN stations on CT were described according to Naruke's lymph node mapping [15].

### 2.4. Clinico-pathologic correlation

All 71 patients had final histologic confirmation of NSCLC by reviewing tissue specimens obtained by resection ($n = 70$) or mediastinoscopy ($n = 1$). Histologic typing was determined according to the World Health Organization classification [16]. The disease stage was based on the TNM classification of the International Union Against Cancer [17].

All resected lymph nodes were formalin-fixed and examined microscopically by hematoxylin and eosin staining. The LN stations on thoracotomy were described according to Naruke's lymph node mapping [15]. To determine histologic causative factors of false PET scans, two authors (K.T. and G.I.) compared PET results and histologic features of LNs by nodal station, and measured the maximum dimension of tumor foci in histologically involved LNs.

Clinical records of each patient were reviewed for age, gender, and a past history of inflammatory disease.

## 3. Results

There were 50 adenocarcinomas, 12 squamous cell carcinomas, five large cell carcinomas, three large cell neuroendocrine carcinomas, and one adenosquamous carcinoma.

FDG-uptake in primary tumors was sufficient in 65 patients and lacking in six. All PET-negative primary tumors were histologically diagnosed as adenocarcinoma with predominant bronchioloalveolar carcinoma (BAC) component, and were pathologic N0 diseases correctly staged as N0 both by CT and PET.

The nodal staging results of CT and FDG PET are presented in Table 1. There were 10 (14%) false-positive PET scans and 14 (20%) false-negative PET scans. Sensitivity, specificity, accuracy, positive predictive value (PPV), and negative predictive value (NPV) for CT were 29, 83, 65, 47, and 70% and for PET were 39, 79, 66, 47, and 73%, respectively.

The CT and FDG PET results of the discrimination between N0/N1 and N2/N3 are presented in Table 2. Sensitivity, specificity, accuracy, positive predictive value, and negative predictive value for CT were 20, 89, 75, 33, and 81% and for PET were 40, 88, 77, 46, and 84%, respectively.

The 10 cases with false-positive PET scan are summarized in Table 3. These patients had FDG uptake in LNs compatible with metastases, but his-

Table 1 Results of nodal staging as the assessment of N1, N2, and N3 lymph nodes on CT and FDG PET

| | Pathologic nodal stage | | |
|---|---|---|---|
| | pN0 | pN1 | pN2 |
| Nodal stage on CT | | | |
| N0 | 39 | 5 | 11 |
| N1 | 2 | 4 | 1 |
| N2 | 3 | 2 | 3 |
| N3 | 0 | 1 | 0 |
| Nodal stage on PET | | | |
| N0 | 38 | 5 | 4 |
| N1 | 3 | 3 | 5 |
| N2 | 0 | 3 | 6 |
| N3 | 3 | 1 | 0 |

Table 2 Results of the discrimination of N0/N1 from N2/N3 on CT and FDG PET

| | Pathologic nodal stage | |
|---|---|---|
| | pN0/pN1 | pN2/pN3 |
| Nodal stage on CT | | |
| N0/N1 | 50 | 12 |
| N2/N3 | 6 | 3 |
| Nodal stage on PET | | |
| N0/N1 | 49 | 9 |
| N2/N3 | 7 | 6 |

tology confirmed no metastatic involvement. The causative factors for false-positive PET scan were: (1) inflammatory conditions (tumor necrosis in two patients, tumor necrosis and obstructive pneumonia in two, LN sarcoid reaction due to previous pulmonary tuberculosis in one (Fig. 1), pulmonary fibrosis in one, rheumatoid arthritis in one); (2) PET mis-localization of an interlobar LN (station #11s) as a mediastinal LN (station #4) in one patient; (3) inability to distinguish the endobronchial polypoid growth of a primary tumor from a lobar LN in one patient (Fig. 2); (4) unknown in one patient. All false-positive LNs due to inflammatory conditions showed reactive lymphoid hyperplasia histologically.

The 14 cases with false-negative PET scan are summarized in Table 4. These patients were found to have LN metastases, despite having PET scans interpreted as negative. The causative factors for false-negative PET scan were: (1) limitation of the spatial resolution of the PET scanner in 12 patients (Fig. 3); (2) PET mis-localization of a mediastinal LN (station #5) as a hilar LN (station #10) in one patient; (3) weak FDG uptake by sporadic microscopic tumor foci due to necrosis with massive bleeding in a metastatic LN in one patient (Fig. 4).

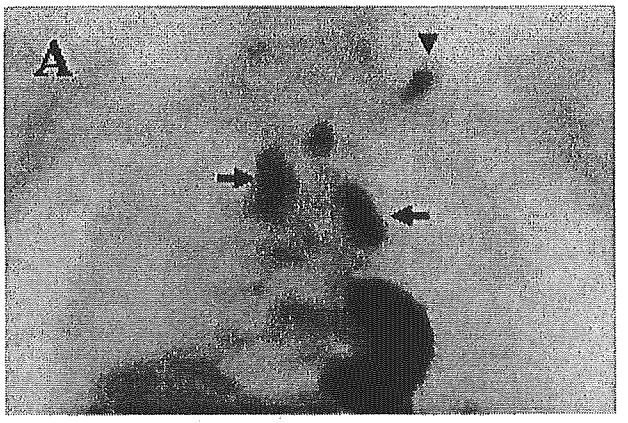


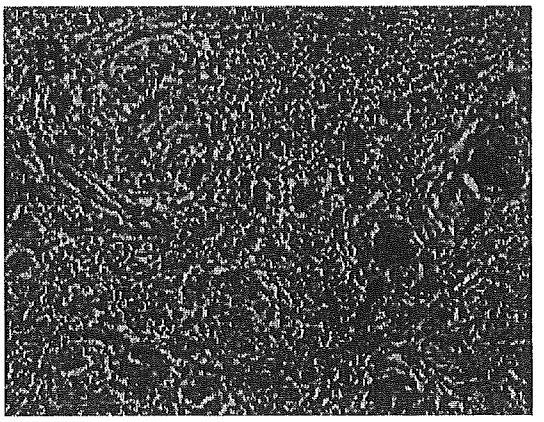

**Fig. 1.** A 64-year-old woman had adenocarcinoma in the left lower lobe, with a past history of pulmonary tuberculosis. CT demonstrated no enlarged lymph nodes. (A) FDG PET (coronal view) demonstrated increased FDG uptake in the bilateral hilar, mediastinal (arrow), and left supraclavicular lymph nodes (arrow head). (B) Enlarged lymph nodes harbored epithelioid granulomas with Langhans-type giant cells (arrow), which were diagnosed as sarcoid reaction (hematoxylin–eosin).

Table 3 False-positive PET scans

| Patient no. | Age/sex | Histology of primary tumor | Location of primary tumor | Nodal stage by CT/PET/pathology | Causative factors |
|---|---|---|---|---|---|
| 1 | 43/F | P/D Ad | Peripheral | N0/N2/N1 | Mis-localization of lymph nodes |
| 2 | 67/F | M/D Ad | Peripheral | N2/N2/N1 | Unknown |
| 3 | 68/M | LCNEC | Peripheral | N0/N3/N0 | Tumor necrosis |
| 4 | 74/F | La | Central | N1/N1/N0 | Endobronchial polypoid growth of a primary tumor |
| 5 | 65/M | La | Central | N3/N2/N1 | Tumor necrosis |
| 6 | 73/M | La | Peripheral | N0/N1/N0 | Tumor necrosis and obstructive pneumonia |
| 7 | 64/F | W/D Ad | Peripheral | N0/N3/N0 | Sarcoid reaction (past history of tuberculosis) |
| 8 | 65/M | M/D Sq | Central | N1/N1/N0 | Tumor necrosis and obstructive pneumonia |
| 9 | 71/F | M/D Ad | Central | N0/N3/N0 | Pulmonary fibrosis |
| 10 | 59/F | M/D Ad | Peripheral | N0/N3/N1 | Rheumatoid arthritis |

W/D: well differentiated; M/D: moderately differentiated; P/D: poorly differentiated.

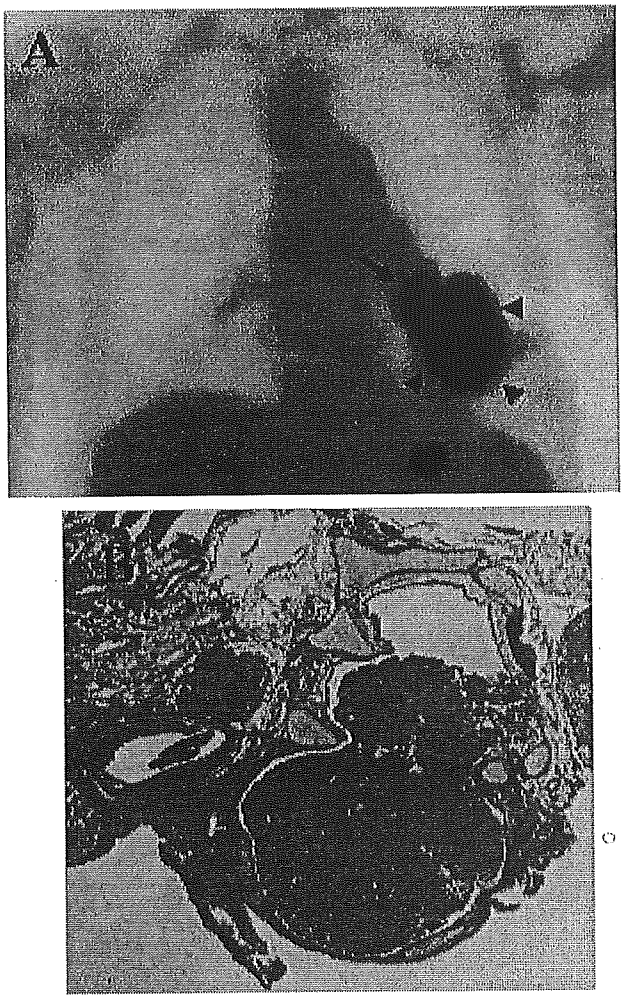


Fig. 2. A 74-year-old woman with large cell carcinoma in the left lower lobe. (A) FDG PET (coronal view) demonstrated increased FDG uptake in the primary tumor (arrow heads) and adjacent lobar lymph node (arrow, PET–N1). (B) Histologically, the involved lobar node on FDG PET corresponded to endobronchial polypoid growth of the primary tumor.

The maximum dimensions of tumor focus in false-negative LNs in group (1) ranged from 1 to 7.5 mm (mean 3.4 mm).

## 4. Discussion

Many retrospective [13,18] and prospective [13,19–21] studies have shown FDG PET to be an accurate imaging modality in the nodal staging of NSCLC. Meta-analytic comparisons of PET and CT [8–11] showed that PET was significantly more accurate than CT in demonstrating nodal metastases. While PET is an important advance in non-invasive staging, it is not perfect. However, few studies have assessed its limitations. In this study, we

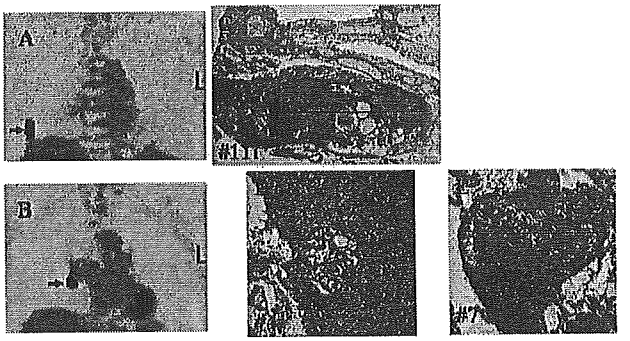


Fig. 3. A 67-year-old man with adenocarcinoma in the right lower lobe. CT demonstrated no enlarged lymph nodes. A FDG PET (coronal view) demonstrated increased FDG uptake in the (A) primary tumor (arrow) and (B) a hilar lymph node (arrow) but not in the mediastinal nodes. The maximum dimensions of tumor focus (black line) in the involved LNs were (C) 16 mm in #11i (PET-positive) (D) 1 mm in #4 (PET-negative), and (E) 4.5 mm in #7 lymph node (PET-negative).

clarified clinico-pathologic factors responsible for false PET results.

We showed that false-positive PET scans were mostly attributable to inflammatory conditions, including tumor necrosis, obstructive pneumonia, previous pulmonary tuberculosis, pulmonary fibrosis, and rheumatoid arthritis. FDG is not a specific marker of malignancy and FDG uptake can be seen at sites of active, acute inflammation, which is due to increased glucose uptake by activated macrophages and inflammatory cells [22]. Inflammatory conditions are well-known factors associated with false-positive PET scans in indeterminate pulmonary nodule evaluation [23]. Roberts et al [12] reported that concurrent inflammatory lung disease and centrally located tumors were causative factors of false-positive PET scans in mediastinal nodal staging in NSCLC. Our results were consistent with these previous findings. Because false-positive populations can benefit from primary surgery, an invasive staging procedure prior to pulmonary resection may be indicated in patients with positive-LN findings on PET, especially those with present or past inflammatory conditions.

FDG PET diagnostic capability is limited not only by cellular activity but also by tumor volume. FDG uptake by small tumor cell focus is often poorly depicted due to partial volume effect. Current PET scanner achieves transaxial resolution of 4–5 mm full-width-half-maximum. A tumor focus smaller than 5 mm may not be detected by current scanners. The maximum dimensions of tumor focus in false-negative LNs ranged from 1 to 7.5 mm (mean 3.4 mm) in our series. The spatial resolution limitations of FDG PET were responsible for 13 of 14 (93%)

Table 4 False-negative PET scans

| Patient no. | Age/Sex | Histology of primary tumor | Location of primary tumor | Nodal stage CT/PET/pathology | Causative factors |
|---|---|---|---|---|---|
| 1 | 59/M | M/D Ad | Peripheral | N0/N0/N2 | Small-sized tumor focus (7.5 mm)[a] |
| 2 | 57/F | P/D Ad | Peripheral | N0/N1/N2 | Mis-localization of lymph nodes |
| 3 | 64/M | M/D Ad | Peripheral | N0/N1/N2 | Small-sized tumor focus (5 mm) |
| 4 | 69/F | M/D Ad | Peripheral | N2/N0/N1 | Small-sized tumor focus (5 mm) |
| 5 | 58/M | M/D Ad | Peripheral | N0/N0/N1 | Small-sized tumor focus (2 mm) |
| 6 | 43/F | M/D Ad | Peripheral | N0/N0/N2 | Small-sized tumor focus (1 mm) |
| 7 | 74/M | M/D Sq | Peripheral | N0/N0/N1 | Small-sized tumor focus (5 mm) |
| 8 | 76/F | M/D Ad | Peripheral | N1/N0/N1 | Small-sized tumor focus (4.5 mm) |
| 9 | 65/M | M/D Sq | Peripheral | N0/N0/N2 | Small-sized tumor focus (4 mm) |
| 10 | 75/M | M/D Sq | Peripheral | N0/N0/N2 | Small-sized tumor focus (2.5 mm) |
| 11 | 73/F | W/D Ad | Central | N0/N0/N1 | Small-sized tumor focus (4 mm) |
| 12 | 67/M | W/D Ad | Peripheral | N0/N1/N2 | Small-sized tumor focus (4.5 mm) |
| 13 | 65/M | M/D Ad | Central | N2/N1/N2 | Weak FDG uptake by microscopic tumor foci in a metastatic LN |
| 14 | 49/M | M/D Ad | Peripheral | N1/N1/N2 | Small-sized tumor focus (2.5 mm) |

W/D: well differentiated; M/D: moderately differentiated; P/D: poorly differentiated.
[a] The maximum dimension of a tumor focus in false-negative lymph nodes are described in parenthesis.

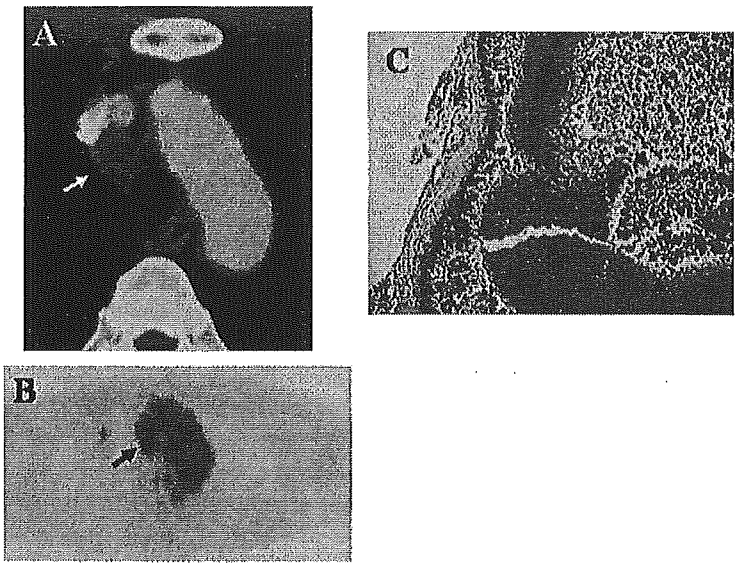


**Fig. 4.** A 65-year-old man with adenocarcinoma in the right upper lobe. (A) CT demonstrated an enlarged pretracheal lymph node with a low density area (arrow). (B) FDG PET (axial view) demonstrated weak FDG uptake at a pretracheal lymph node (arrow). (C) Histologically, the pretracheal lymph node showed scattered microscopic tumor foci (arrow heads) in an area of necrosis with massive bleeding.

false-negative PET results in the present study. FDG PET is not reliable in diagnosing small tumor foci in LNs. The rewarding prognosis after straightforward resection in patients with minimal N2 disease (no mediastinal LN enlargement on CT), compared to those with clinical N2 disease (mediastinal LN enlargement on CT) is well documented [24,25]. Because most false-negative LNs in our study had tiny tumor foci 5 mm or less in size and were not enlarged on CT, fair prognosis after surgical resection can be expected. False-negative PET results might not be clinically relevant.

Another disadvantage of FDG PET is its limited anatomical resolution due to the paucity of anatomic information in metabolic images [21]. Although PET-positive LNs were localized referring to contrast-enhanced CT findings in this study, it was hard to distinguish hilar LNs from adjacent me-

diastinal LNs in two cases (one false-positive and one false-negative PET scans). In another case, we could not discriminate endobronchial polypoid tumor growth from a lobar LN. New PET–CT fusion systems may enable more precise anatomic localization [26–28].

Our estimates in the diagnostic accuracy of PET for LN staging in NSCLC patients may be biased. Our study resulted in a sensitivity of 39%, specificity of 79%, and accuracy of 66%, and did not show the superiority of PET over CT. Our sensitivity lower than many prospective studies [13,19–21] and meta-analyses [8–11] may be attributable to several factors. First, our patient population, the majority of which (55/71) had no enlarged LN on CT, might be biased. Most involved mediastinal nodes were not enlarged, which may explain too many false-negatives. Second, our method of FDG PET may not be optimal in the following points: (1) allowing patients with serum glucose values up to 150 mg/dl (2) rather low injected dose of FDG, and (3) interpretation of images on hard copy films. Third, the definition of nodal staging accuracy of PET used in our study was different from that in previous studies. We defined accurate staging as correct localization of involved N1, N2, and N3 nodes. This was because we compared PET staging results and histologic findings to determine pathologic factors responsible for false PET results. In most previous studies, however, accurate LN staging was defined as correct discrimination between N0/N1 and N2/N3. This is reasonable because mediastinal node involvement diagnosis is important in treatment strategy decision making. So, we also evaluated nodal staging accuracy as correct discrimination between N0/N1 and N2/N3. Although the specificity and NPV increased, sensitivity and PPV were almost the same. This may be attributable to the low pathologic N2 prevalence (21%) in our study population. Phillips et al [29] reported that as prevalence of disease decreases, the reliability of a positive result will drop, and the reliability of a negative result will increase. High NPV of PET in diagnosing mediastinal node involvement may warrant mediastinoscopy omission.

Although the majority of lung cancer shows increased FDG uptake, BAC has been reported to be often negative on FDG PET [30,31]. In our study, all PET-negative primary tumors were adenocarcinomas with predominant BAC component. BAC predominant adenocarcinomas rarely have lymph node metastases and distant metastases [32,33]. They are reliably diagnosed on thin-section CT scan, because they are depicted as ground glass opacity [34]. These adenocarcinomas may not be indicated for preoperative PET examinations for the characteristics.

In summary, inflammatory conditions were most responsible for false-positive PET scans, and spatial resolution limitation of FDG PET was the causative factor of false-negative PET scans. A positive PET scan cannot guarantee a pathologic positive LN, and a negative PET scan cannot guarantee a pathologic negative LN. Recognizing these factors in advance would be clinically helpful in accurate nodal staging with FDG PET.

## Acknowledgments

We thank Prof. J. Patrick Barron, International Medical Communications Center, Tokyo Medical University, for reviewing the English manuscript. This study was supported in part by a Grant-in-Aid for Cancer Research from the Ministry of Health and Welfare, Japan.

## References

[1] McKenna Jr RJ, Libshitz HI, Mountain CE, McMurtrey MJ. Roentgenographic evaluation of mediastinal nodes for preoperative assessment in lung cancer. Chest 1985;88:206–10.

[2] McLoud TC, Bourgouin PM, Greenberg RW, Kosiuk JP, Templeton PA, Shepard JA, et al. Bronchogenic carcinoma: analysis of staging in the mediastinum with CT by correlative lymph node mapping and sampling. Radiology 1992;182:319–23.

[3] Gross BH, Glazer GM, Orringer MB, Spizarny DL, Flint A. Bronchogenic carcinoma metastatic to normal-sized lymph nodes: frequency and significance. Radiology 1988;166:71–4.

[4] Libshitz HI, McKenna Jr RJ, Haynie TP, McMurtrey MJ, Mountain CT. Mediastinal evaluation in lung cancer. Radiology 1984;151:295–9.

[5] Takamochi K, Nagai K, Yoshida J, Suzuki K, Ohde Y, Nishimura M, et al. The role of computed tomographic scanning in diagnosing mediastinal node involvement in non-small cell lung cancer. J Thorac Cardiovasc Surg 2000;119:1135–40.

[6] Takamochi K, Nagai K, Suzuki K, Yoshida J, Ohde Y, Nishiwaki Y. Clinical predictors of N2 disease in non-small cell lung cancer. Chest 2000;117:1577–82.

[7] Gallagher BM, Fowler JS, Gutterson NI, MacGregor RR, Wan CN, Wolf AP. Metabolic trapping as a principle of oradiopharmaceutical design: some factors resposible for the biodistribution of [18F] 2-deoxy-2-fluoro-d-glucose. J Nucl Med 1978;19:1154–61.

[8] Dwamena BA, Sonnad SS, Angobaldo JO, Wahl RL. Metastases from non-small cell lung cancer: mediastinal staging in the 1990s—meta-analytic comparison of PET and CT. Radiology 1999;213:530–6.

[9] Toloza EM, Harpole L, McCrory DC. Non-invasive staging of non-small cell lung cancer: a review of the current evidence. Chest 2003;123:137S–46S.

[10] Gould MK, Kuschner WG, Rydzak CE, Maclean CC, Demas AN, Shigemitsu H, et al. Test performance of positron emis-

sion tomography and computed tomography for mediastinal staging in patients with non-small-cell lung cancer: a meta-analysis. Ann Intern Med 2003;139:879–92.
[11] Hellwig D, Ukena D, Paulsen F, Bamberg M, Kirsch CM. Meta-analysis of the efficacy of positron emission tomography with F-18-fluorodeoxyglucose in lung tumors. Basis for discussion of the German Consensus Conference on PET in Oncology. Pneumologie 2001;55:367–77.
[12] Roberts PF, Follette DM, von Haag D, Park JA, Valk PE, Pounds TR, et al. Factors associated with false-positive staging of lung cancer by positron emission tomography. Ann Thorac Surg 2000;70:1154–9 (discussion 9-60).
[13] Gupta NC, Tamim WJ, Graeber GG, Bishop HA, Hobbs GR. Mediastinal lymph node sampling following positron emission tomography with fluorodeoxyglucose imaging in lung cancer staging. Chest 2001;120:521–7.
[14] Patz Jr EF, Lowe VJ, Goodman PC, Herndon J. Thoracic nodal staging with PET imaging with 18FDG in patients with bronchogenic carcinoma. Chest 1995;108:1617–21.
[15] Naruke T, Suemasu K, Ishikawa S. Lymph node mapping and curability at various levels of metastasis in resected lung cancer. J Thorac Cardiovasc Surg 1978;76:832–9.
[16] World Health Organization, Histological Typing of Lung and Pleural Tumours. 3rd ed. New York: Springer-Verlag, 1999.
[17] Mountain CF. Revisions in the International System for Staging Lung Cancer. Chest 1997;111:1710–7.
[18] Marom EM, McAdams HP, Erasmus JJ, Goodman PC, Culhane DK, Coleman RE, et al. Staging non-small cell lung cancer with whole-body PET. Radiology 1999;212:803–9.
[19] Pieterman RM, van Putten JW, Meuzelaar JJ, Mooyaart EL, Vaalburg W, Koeter GH, et al. Preoperative staging of non-small-cell lung cancer with positron-emission tomography. N Engl J Med 2000;343:254–61.
[20] Vansteenkiste JF, Stroobants SG, De Leyn PR, Dupont PJ, Bogaert J, Maes A, et al. Lymph node staging in non-small-cell lung cancer with FDG-PET scan: a prospective study on 690 lymph node stations from 68 patients. J Clin Oncol 1998;16:2142–9.
[21] Valk PE, Pounds TR, Hopkins DM, Haseman MK, Hofer GA, Greiss HB, et al. Staging non-small cell lung cancer by whole-body positron emission tomographic imaging. Ann Thorac Surg 1995;60:1573–81 (discussion 81–82).
[22] Kubota R, Kubota K, Yamada S, Tada M, Ido T, Tamahashi N. Microautoradiographic study for the differentiation of intratumoral macrophages, granulation tissues and cancer cells by the dynamics of fluorine-18-fluorodeoxyglucose uptake. J Nucl Med 1994;35:104–12.
[23] Dewan NA, Gupta NC, Redepenning LS, Phalen JJ, Frick MP. Diagnostic efficacy of PET-FDG imaging in solitary pulmonary nodules. Potential role in evaluation and management. Chest 1993;104:997–1002.
[24] Andre F, Grunenwald D, Pignon JP, Dujon A, Pujol JL, Brichon PY, et al. Survival of patients with resected N2 non-small-cell lung cancer: evidence for a subclassification and implications. J Clin Oncol 2000;18:2981–9.
[25] Suzuki K, Nagai K, Yoshida J, Nishimura M, Takahashi K, Nishiwaki Y. The prognosis of surgically resected N2 non-small cell lung cancer: the importance of clinical N status. J Thorac Cardiovasc Surg 1999;118:145–53.
[26] Aquino SL, Asmuth JC, Moore RH, Weise SB, Fischman AJ. Improved image interpretation with registered thoracic CT and positron emission tomography data sets. AJR Am J Roentgenol 2002;178:939–44.
[27] D'Amico TA, Wong TZ, Harpole DH, Brown SD, Coleman RE. Impact of computed tomography-positron emission tomography fusion in staging patients with thoracic malignancies. Ann Thorac Surg 2002;74:160–3 (discussion 3).
[28] Lardinois D, Weder W, Hany TF, Kamel EM, Korom S, Seifert B, et al. Staging of non-small-cell lung cancer with integrated positron-emission tomography and computed tomography. N Engl J Med 2003;348:2500–7.
[29] Phillips WC, Scott JA, Blasczcynski G. Statistics for diagnostic procedures. I. How sensitive is "sensitivity"; how specific is "specificity"? AJR Am J Roentgenol 1983;140:1265–70.
[30] Higashi K, Ueda Y, Seki H, Yuasa K, Oguchi M, Noguchi T, et al. Fluorine-18-FDG PET imaging is negative in bronchioloalveolar lung carcinoma. J Nucl Med 1998;39:1016–20.
[31] Kim BT, Kim Y, Lee KS, Yoon SB, Cheon EM, Kwon OJ, et al. Localized form of bronchioloalveolar carcinoma: FDG PET findings. AJR Am J Roentgenol 1998;170:935–9.
[32] Higashiyama M, Kodama K, Yokouchi H, Takami K, Mano M, Kido S, et al. Prognostic value of bronchiolo-alveolar carcinoma component of small lung adenocarcinoma. Ann Thorac Surg 1999;68:2069–73.
[33] Takamochi K, Yoshida J, Nishimura M, Yokose T, Sasaki S, Nishiwaki Y, et al. Prognosis and histologic features of small pulmonary adenocarcinoma based on serum carcinoembryonic antigen level and computed tomographic findings. Eur J Cardiothorac Surg 2004;25:877–83.
[34] Kuriyama K, Seto M, Kasugai T, Higashiyama M, Kido S, Sawai Y, et al. Ground-glass opacity on thin-section CT: value in differentiating subtypes of adenocarcinoma of the lung. AJR Am J Roentgenol 1999;173:465–9.

*Jpn J Clin Oncol 2005;35(1)37–39*
*doi:10.1093/jjco/hyi002*

Case Reports

# Multiple Sclerosing Hemangiomas with a 10-year History

**Tomoyuki Hishida[1], Junji Yoshida[1], Mitsuyo Nishimura[1], Genichiro Ishii[2], Yutaka Nishiwaki[1] and Kanji Nagai[1]**

[1]Divison of Thoracic Oncology, National Cancer Center Hospital East, Kashiwa, Chiba and [2]Pathology Division, National Cancer Center Research Institute East, Kashiwa, Chiba, Japan

Received July 6, 2004; accepted August 22, 2004

We report a case of multiple sclerosing hemangiomas arising in a 38-year-old woman. Computed tomography (CT) scans of the chest showed multiple small nodules in all lobes of the right lung. The nodule sizes ranged from a few millimeters to the largest of 3.1 cm, which was located in the right middle lobe. She underwent right middle lobectomy to confirm the histological diagnosis. The resected specimen revealed multiple sclerosing hemangiomas. We followed this patient by annual chest CT scans for 10 years and demonstrated that all residual nodules remained unchanged. This is the first report of stable multiple pulmonary sclerosing hemangiomas observed for such a long period.

*Key words: sclerosing hemangioma – multiple – lung*

## INTRODUCTION

Pulmonary sclerosing hemangioma is a rare lung neoplasm usually presenting as a peripheral and solitary nodule of less than 3 cm in diameter, predominantly in asymptomatic middle-aged women (1,2). The clinical course of sclerosing hemangioma is usually slow and benign. However, as they are extremely rare manifestations, their natural course has not been well understood.

## CASE REPORT

A 38-year-old asymptomatic woman underwent chest roentography for preoperative evaluation of bartholinitis. Multiple small nodules were pointed out in the right lung field, and she was referred to our institution for further examinations. Computed tomography (CT) scans of the chest showed innumerable lesions varying from several millimeters to 3.1 cm in diameter in all lobes of the right lung but none in the left lung. Each lesion was a round-shaped nodule with a distinct margin and homogeneous density. The largest lesion, measuring 3.1 cm × 2.9 cm, was depicted in the right middle lobe accompanied by numerous tiny nodules (Fig. 1). In the right upper and lower lobes, multiple nodules of various sizes were present. No lymphadenopathy was observed. Bronchoscopic examinations failed to obtain sufficient material because of massive bleeding from the largest middle lobe lesion. She underwent right middle lobectomy in September 1993 in order to confirm the histological diagnosis. She was discharged without any complications on the seventh postoperative day.

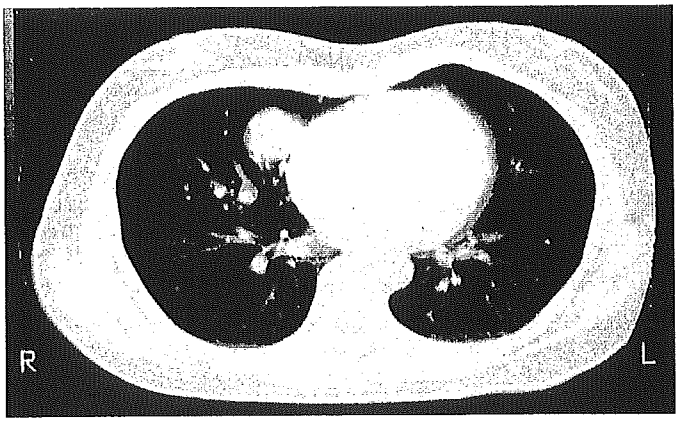


**Figure 1.** Preoperative CT scans shows the largest nodule, measuring 3.1 cm × 2.9 cm in size, accompanied by numerous tiny nodules in the right middle lobe of the lung.

Macroscopically, a well-circumscribed nodule measuring 2.7 cm × 2.7 cm in size was located in the right middle lobe of the resected specimen. Scattered around the main nodule were observed innumerable minute nodules of various sizes. They were well-circumscribed but not encapsulated. Microscopically, each nodule was composed of a variable proportion of four patterns: solid, hemorrhagic, sclerotic and papillary. Smaller lesions, particularly minute ones, were

For reprints and all correspondence: Kanji Nagai, Division of Thoracic Oncology, National Cancer Center Hospital East, 6-5-1, Kashiwanoha, Kashiwa, Chiba 277-8577, Japan. E-mail: knagai@east.ncc.go.jp

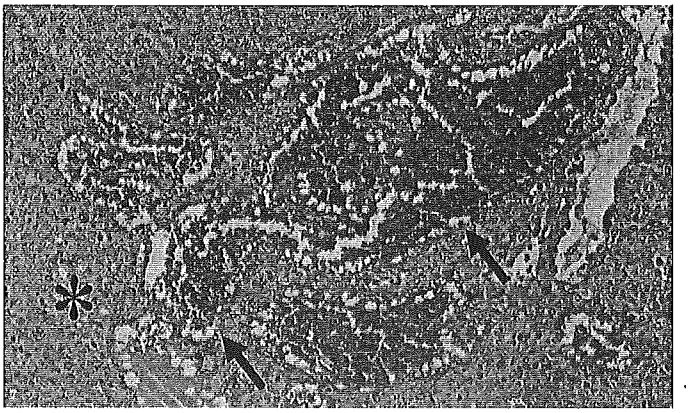

**Figure 2.** In the solid component, round cells with pale cytoplasm demonstrate a sheet-like proliferation (asterisk). In the hemorrhagic component, blood-filled spaces are lined by cuboidal surface cells (arrow).

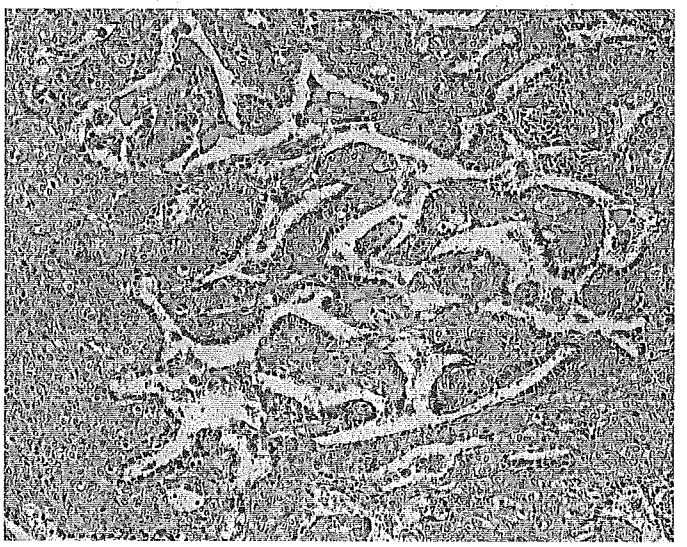

**Figure 3.** In a small portion of the tumor, the papillary pattern composed of cuboidal surface cells is present within the solid component.

mainly of solid and hemorrhagic patterns. The solid pattern was composed of a sheet-like proliferation of round to polygonal cells with pale cytoplasm. In the hemorrhagic pattern, red blood cells were accumulated within cystic spaces composed of cuboidal surface cells (Fig. 2). In a small portion of the tumor, the papillary pattern composed of cuboidal surface cells was observed within the solid proliferation of round tumor cells (Fig. 3). The sclerotic pattern was scarcely present. Based on these histological findings, we diagnosed these lesions as multiple sclerosing hemangiomas of the lung.

Postoperatively, the patient visited our outpatient clinic at 6-month intervals for 3 years and at 1-year intervals thereafter for 7 years. We have been following up residual lesions located in the right upper and lower lobes by chest roentography at every visit and annual chest CT scans. Figure 4a and b shows the comparative CT scans of the right lower lobe lesions taken in March 1995 (about 18 months after surgery) and in March 2004 (about 10 and a half years after surgery). There was neither nodule growth nor new lesions.

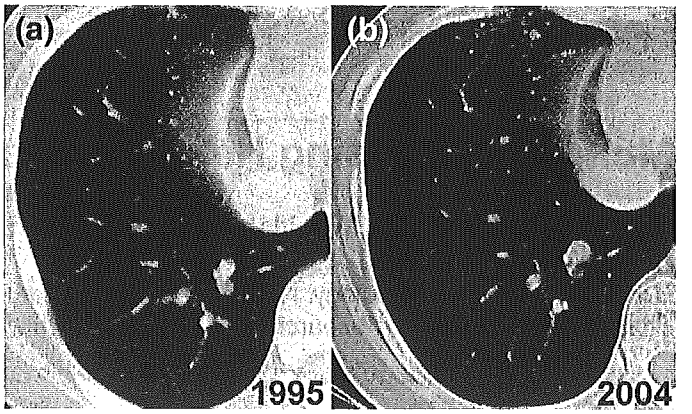


**Figure 4.** Comparative CT scans of the nodules located in the right lower lobe in March 1995 (**a**) and in March 2004 (**b**). Scattered small nodules remain unchanged.

## DISCUSSION

Sclerosing hemangioma of the lung is a relatively rare benign tumor first described by Liebow and Hubell in 1956 (1). Histologically, there is a mixture of solid, sclerotic, papillary and hemorrhagic components in typical cases. In each component, two populations of cells can be identified: solid-growing polygonal round cells with pale cytoplasm and cuboidal surface cells covering papillary structures (2). Recent studies suggest that sclerosing hemangioma derives from primitive respiratory epithelium and demonstrates neoplastic differentiation (3,4). The majority of pulmonary sclerosing hemangiomas present as a solitary pulmonary nodule, whereas multiple lesions are reported to account for 4% of all cases (2,3). Because of its rarity, the natural course of pulmonary multiple sclerosing hemangiomas has not been well understood.

CT findings of residual nodules in the present case were very similar to resected nodules, and the resected middle lobe contained numerous foci of sclerosing hemangiomas. Therefore, we believe residual scattered nodules are multiple sclerosing hemangiomas, although cytopathological evidence was not obtained. It has not been fully studied whether the multiplicity of multiple sclerosing hemangiomas suggests a progressive clinical course or not.

As we reviewed the literature, although a solitary pulmonary sclerosing hemangioma that showed rapid progression was reported (5), multiple lesions previously reported have all been slow-growing cases. Hayashi and colleagues followed a patient with gradually growing multiple pulmonary sclerosing hemangiomas for as long as 7 years before surgical resection (6). Lee and coworkers followed a case of bilateral multiple (four) sclerosing hemangiomas of the lung, which grew slowly (7). We have followed the present case intensively